18 Physical Properties of Magnetic Gels

Helmut R. Brand, Philippe Martinoty, and Harald Pleiner

in *Cross-Linked Liquid Crystalline Systems: From Rigid Polymer Networks to Elastomers*,
eds. G. Crawford, D. Broer, and S. Zumer (Taylor and Francis, 2011) ISBN: 978-1-4200-4622-9.

CONTENTS

18.1 INTRODUCTION AND HISTORICAL OVERVIEW

While liquid crystalline elastomers combining the properties of liquid crystals and of elastomers, have been synthesized first in Finkelmann's group over 25 years ago [1] (compare Ref. [2] for a recent review of some macroscopic properties), the field of magnetic gels is much more recent. About a decade ago, Zrinyi's group reported the preparation of isotropic magnetic gels combining the properties of a gel with those of a magnetic liquid [3, 4].

Since the late 90's, isotropic magnetic gels, which only react to magnetic field gradients, but not to homogeneous magnetic fields, have been investigated in detail synthetically, experimentally and theoretically [5–25], where a large body of work has been accumulated in particular by Zrinyi's group. In particular Ref. [5] gives a concise and clear overview of the early work on isotropic magnetic gels. Apart from combining ferrofluids and polymer networks, other groups have generated magnetic gels by embedding ferrite particles or $\gamma - Fe_2O_3$ particles of nanometer scale into a gel matrix [26–30]. When magneto-rheological fluids are combined with a polymer network, magneto-rheological gels result [31–37].

In 2003 the groups of Martinoty [38] and Zrinyi [39] pioneered the synthesis and characterization of uniaxial magnetic gels by generating the magnetic gel in an external magnetic field thus freezing-in the direction of the external magnetization. In contrast to isotropic magnetic gels, which respond only to field gradients, uniaxial magnetic gels can be oriented in a homogeneous magnetic field [38]. While the static properties of iron and magnetite particles containing magnetic gels have been elucidated in Zrinyi's group [39–44], Martinoty's group has focused on the investigation of the dynamic properties, in particular using piezorheometry. Very recently, Martinoty's group [45] has also studied the magnetic-field induced generation of a novel uniaxial magneto-rheological system - using a magneto-rheological fluid -, which is solid-like in the field direction and liquid-like transverse to the direction of the external field. Correspondingly, the review and the analysis of the physical properties of uniaxial magnetic gels comprises the major part of this chapter.

We note that very recently also the synthesis and characterization of thermoreversible ferrogels has been reported [46]. In these systems the sol - gel transition can be observed as a function of temperature. It will be clearly very interesting to study the rheological behavior and the instabilities (e.g., the Rosensweig instability) in these systems using the temperature as a continuously variable parameter.

In the next Section we present a detailed analysis of the available experimental investigations of uniaxial magnetic gels followed by a Section describing the macroscopic properties and novel cross-coupling effects for both, isotropic and uniaxial magnetic gels [18, 47–49]. In this Section we make use of the approach of hydrodynamics and macroscopic dynamics, which is valid in the low frequency, long wavelength limit (cf. [50] for a detailed exposition of the methods). In the last Section we discuss similarities and differences in the physical, in particular in the macroscopic properties between magnetic gels on the one hand and liquid crystalline gels and elastomers on the other.

18.2 EXPERIMENTAL ASPECTS

18.2.1 INTRODUCTION

Magnetic gels or elastomers are composite materials made up of magnetic particles embedded in a polymeric matrix. Like liquid crystalline elastomers, they belong to the category of systems known as 'intelligent'. They are called uniaxial when the magnetic particles are oriented in a permanent way in a given direction. The interest of the latter systems is that they respond not only to gradients of the magnetic field, like superparamagnetic gels, but also to uniform magnetic fields.

In this Section, we concentrate on the main experimental results obtained for uniaxial magnetic gels and elastomers. We address three fundamental problems raised by these materials: the mechanical anisotropy, the influence of an external magnetic field on the mechanical anisotropy and the formation kinetics governing the properties of the final material. These topics will be discussed in the light of the experiments performed by the groups of Zrinyi and Martinoty. The static aspects, mainly studied by Zrinyi's group, and the dynamic aspects studied by Martinoty's group will be presented separately.

18.2.2 STATIC ASPECTS

In the experiments performed by Zrinyi's group [40–42], two different types of systems were investigated:

a) Magnetic elastomers composed of poly(dimethyl siloxane) (PDMS) networks filled either with carbonyl iron particles, or with Fe_3O_4 particles (magnetite particles). As shown in Figure 18.1, the carbonyl iron particles are polydisperse and have spherical shape with smooth surface, in contrast to the magnetite particles. The concentration of the filler particles in the elastomer varied from 10 to 40 wt%.

b) Magnetic gels composed of poly(vinyl alcohol) (PVA) hydrogels filled with magnetite particles whose concentration in the gel was 1.2 wt%.

The uniaxial samples were prepared by applying a uniform magnetic field during the formation process. To do that, the mixture containing the polymeric matrix and the magnetic particles was introduced into a cube-shape mould placed between the poles of an electromagnet. The formation of the uniaxial gel or elastomer proceeds in two steps. First, the embedded magnetic particles are aligned along a common direction, leading to fiber formation. The aligned particles are then locked by the chemical cross-linking, giving rise to a highly anisotropic material. For detail about the preparation of the sample see [40–42].

An example of the texture of the final material is given by observations using an optical microscope performed on a uniaxial magnetic PVA hydrogel prepared by Martinoty's group (see Section 18.2.3.4.2 dealing with dynamic aspects; Figure 18.10).

18.2.2.1 Shear mechanical anisotropy

In [40–42], the static shear modulus G was determined by applying a unidirectional compression force on the sample and by measuring the resulting stress-strain relationship. G is then deduced from the neo-Hookean law of rubber elasticity [51], which is given by:

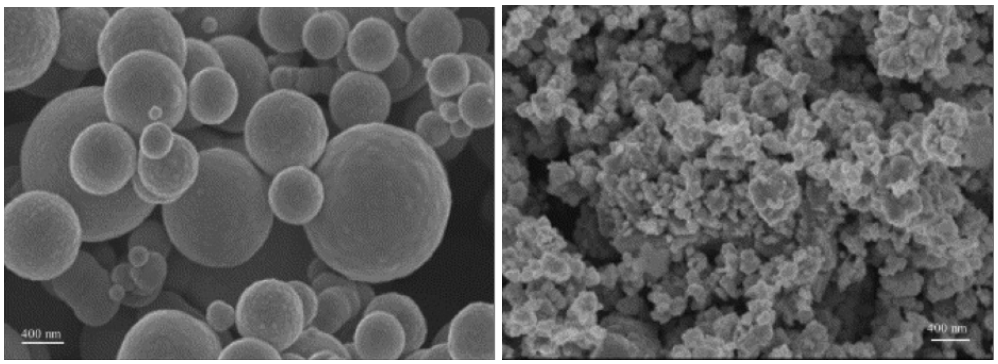

Figure 18.1: SEM pictures of the iron (a) and magnetite particles (b). The bar corresponds to 400 nm. (Reprinted from Varga, Z., Filipcsei, G., and Zrinyi, M., *Polymer*, 46, 7779, 2005. Copyright 2005, with permission from Elsevier).

$$\sigma_n = G(\lambda - \lambda^{-2}) \tag{18.1}$$

σ_n is the nominal stress defined as the ratio f/S where f is the tensile force and S the cross-Sectional area of the sample measured in the undeformed state. λ is the compression ratio l/l_0 where l corresponds to the length of the sample measured in the direction of the force, and l_0 is the initial length associated with the undeformed state.

All the measurements were made at room temperature on samples containing a high concentration of magnetic particles varying from 10% to 40% in weight. The results obtained for a uniaxial PDMS sample filled with 40 wt % magnetite particles and for its isotropic analogue are shown in Figure 18.2. For each of the three distributions of the magnetic particles with respect to the applied force, the data clearly show that the stress-strain behavior obeys Equation 18.1. The significant differences in the slopes of the stress-strain curves demonstrate that G is very sensitive to the spatial distribution of the magnetite particles. In particular, the uniaxial sample exhibits highly anisotropic properties with a $\sim 70\%$ anisotropy in G. Similar types of behavior are observed for the other concentrations.

The situation is not the same when the PDMS elastomer is filled with iron particles. Two cases must be considered, according to whether the direction of the applied compression force is parallel or perpendicular to the fiber structure. For the perpendicular case, the stress-strain behavior roughly obeys the ideal behavior given by Equation 18.1. This is no longer the case when the direction of the compression force is parallel to the fiber structure, and a strong deviation from the ideal behavior is observed, as shown in Figure 18.3. This striking change in behavior for the parallel geometry between the iron-filled samples and the magnetite-filled samples indicates that the interaction of the particles with the polymeric matrix is different. As we will see below, the data obtained at large deformations lead to the same conclusion.

Since the elastic modulus is related to the degree of swelling, the anisotropy in the mechanical behavior can also be observed in swelling experiments. The data of Fig 18.4, taken for a PDMS elastomer filled with 40 wt% magnetite particles, show that the swelling is

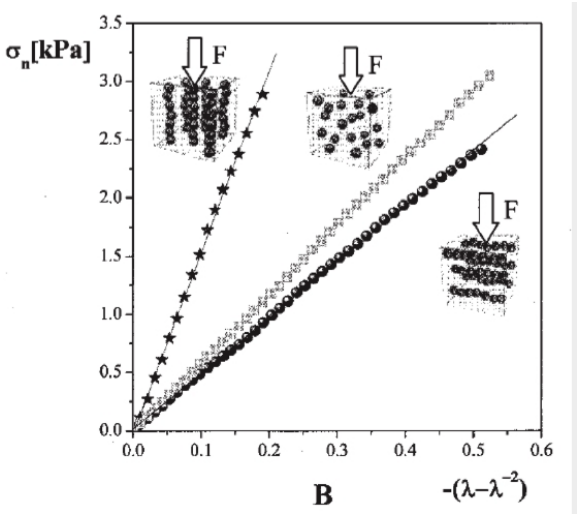

Figure 18.2: Stress-strain behavior of PDMS elastomers filled with 40 wt % magnetite particles for three different spatial distributions of the particles. The white arrows indicate the direction of the applied compression force. (Varga, Z. et al. *Macromol. Symp.*, 227, 123, 2005. CopyrightWiley-VCH Verlag GmbH & Co. KGaA. Reproduced with permission.)

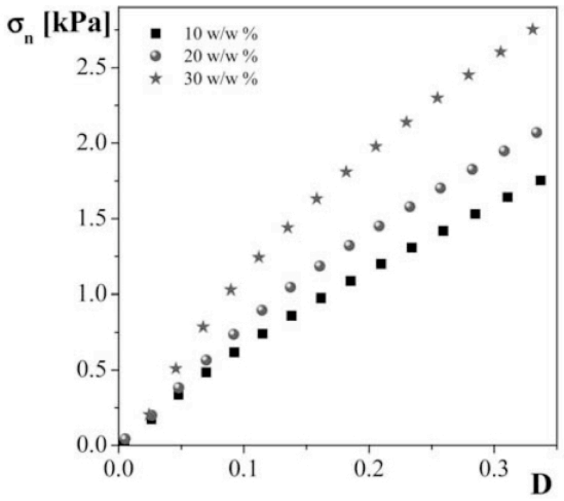

Figure 18.3: Stress-strain behavior of a uniaxial magnetic PDMS elastomer filled with iron particles. The compression force is parallel to the direction of the fibers. The symbols indicate the concentrations of particles. A 400 mT uniform magnetic field was applied during the formation of the sample. $D = \lambda - \lambda^{-2}$. (Reprinted fromVarga, Z., Filipcsei, G., and Zrinyi, M., *Polymer*, 46, 7779, 2005. Copyright 2005, with permission from Elsevier.)

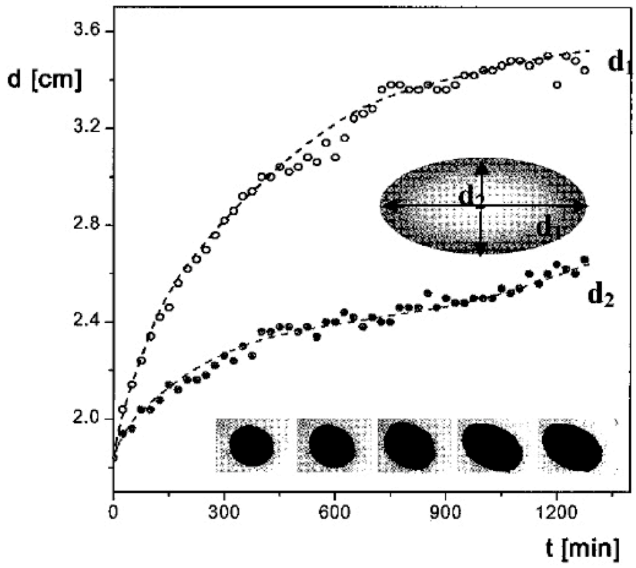

Figure 18.4: Anisotropic swelling of a uniaxial magnetic PDMS gel filled with 40 wt% magnetite particles in n-hexane. (Reprinted from Varga, Z., Filipcsei, G., and Zrinyi, M., *Polymer*, 46, 7779, 2005. Copyright 2005, with permission from Elsevier.)

anisotropic, indicating again the anisotropic nature of the material.

All the previous experiments concern the behavior at small deformations. New effects appear at large deformations, as we will see now. Figure 18.5 shows the stress-strain curves taken for the uniaxial PVA gel loaded with magnetite particles, and for its isotropic analogue. In all cases, it can be seen that the data taken at large deformations deviate from the linear behavior observed at small deformations. Particularly interesting is the situation where the applied force is parallel to the fibers. In that case a bending occurs below a critical strain. This effect, which reflects a stress induced softening, has been interpreted as a mechanical instability associated with the buckling of the fibers [41]. Similar types of behavior were observed for the PDMS elastomer loaded with magnetite particles.

Figure 18.6 shows the data obtained on the iron-filled PDMS elastomer. As it can be seen, the shape of the stress-strain curves is different from those observed in the systems filled with magnetite particles (PVA gel or PDMS elastomer). In the case where the applied force is parallel to the fibers, the compression of the sample induces a break point in the stress-strain curve instead of a softening. According to [41], this break point reflects the destruction of the fiber structure of the iron particles.

The difference in behavior between the magnetite-loaded and the iron-loaded systems can be explained by the fact that the iron particles do not interact strongly with the polymer network, contrary to the magnetite particles. As a result, the polymer network cannot prevent the break-up of the iron fiber structure under compression, while it prevents the destruction

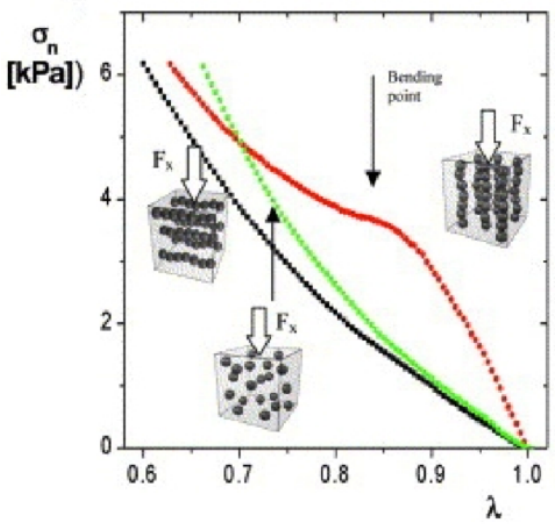

Figure 18.5: Stress-strain curves of magnetite-loaded PVA gels for three different spatial distributions of the particles but with the same concentration of magnetite particles. The white arrows indicate the direction of the applied compression force. A 400 mT uniform magnetic field was applied during the formation of the sample. (Reprinted from Varga, Z., Filipcsei, G., and Zrinyi, M., *Polymer*, 46, 7779, 2005. Copyright 2005, with permission from Elsevier.)

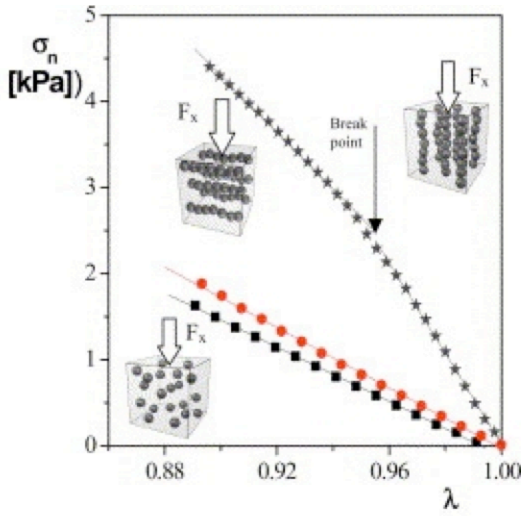

Figure 18.6: Same as in Figure 18.5, but for iron-loaded PDMS elastomers. (Reprinted from Varga, Z., Filipcsei, G., and Zrinyi, M., *Polymer*, 46, 7779, 2005. Copyright 2005, with permission from Elsevier.)

of the magnetite fibers. As already stressed above, the nature of the magnetic particles (magnetite versus iron), and probably their size (larger for the iron particles than for the magnetite particles), their shape and geometric features (spherical shape with smooth surface for the iron particles, irregular angular shape with sharp facets for magnetite particles) play a major role in the mechanical behavior of both systems.

18.2.2.2 Influence of an external magnetic field on the behavior of the shear modulus G

Since the shape of the uniaxial elastomers is coupled to the magnetic field through the magnetic particles, it is interesting to investigate the influence of a uniform external field, H, on the behavior of G. This has been done in [42] on uniaxial (PDMS) elastomers filled with carbonyl iron particles. The experiments were performed as a function of particle concentration, intensity of the magnetic field and of the spatial distribution of the particles. By varying the direction of the magnetic field with respect to the direction of the fibers and to the direction of the compression stress, five different geometries were studied. In all cases an increase of G was found with increasing H. However, this magnetic reinforcement effect is only significant when the applied field is parallel to the fibers. This is not too surprising since in this case the magnetic field reinforces the rigidity of the fibers. Typical results are shown in Figure 18.7 for the two geometries where the field is applied in a direction parallel to the fibers. It can be seen that the largest increase in G is observed when the magnetic field is parallel to both the particle alignment and the applied force.

It was found that the magnetically induced excess modulus, G_M^E, is proportional to H^2 at weak fields. To take into account this limiting behavior and the fact that G_M^E approaches a saturation value at high fields, the G_M^E data have been analyzed with the following equation

$$G_M^E(H) = G_{M,\infty} \frac{H^2}{a_B + H^2} \tag{18.2}$$

where a_B is a material parameter and $G_{M,\infty}$ the value at high field. This equation provides a good fit to the experimental data, as shown by Figure 18.8.

As will be shown in the next Section this magnetic field induced enhancement is not due to static magnetostriction effects, but rather associated with the magnetic field dependence of the elastic moduli.

18.2.3 DYNAMIC ASPECTS

18.2.3.1 Introduction

Contrary to the static aspects, the dynamic aspects of uniaxial magnetic gels have practically never been studied, essentially because conventional rheometers do not allow taking measurements in the presence of a magnetic field. The piezorheometer developed in Martinoty's group over the last few years makes it possible to perform these measurements. In this technique, the gels are formed directly in the measuring cell which, due to its reduced dimensions, can be placed in the air-gap of an electromagnet. This makes it possible to follow the kinetics

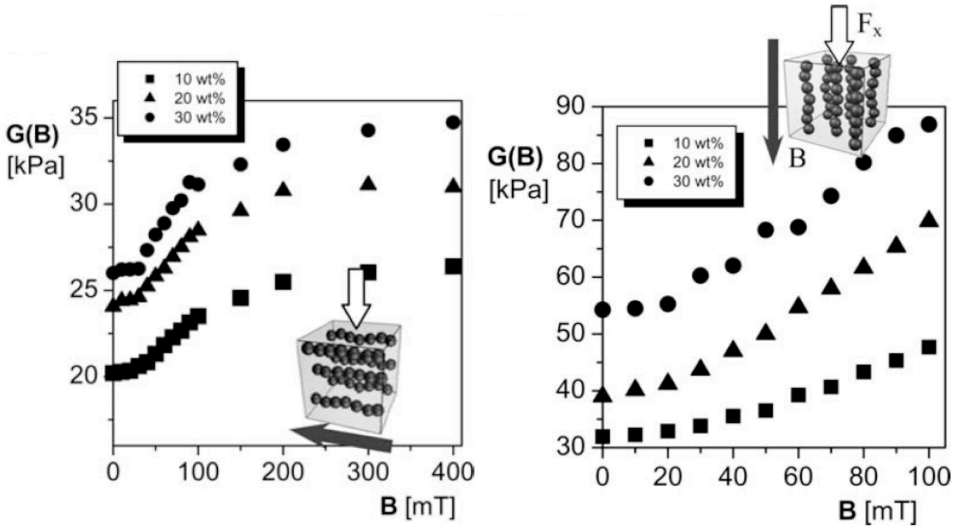

Figure 18.7: Influence of a uniform magnetic field intensity on the elastic modulus of a uniaxial iron-loaded PDMS elastomer. The white and black arrows indicate the direction of the applied force and of the external magnetic field, respectively. Left: The force is applied perpendicularly to the magnetic field. Right: The applied force and the applied magnetic field are parallel. The symbols indicate the concentration of iron particles. (Reprinted from Varga, Z., Filipcsei, G., and Zrinyi, M., *Polymer*, 46, 7779, 2005. Copyright 2005, with permission from Elsevier.)

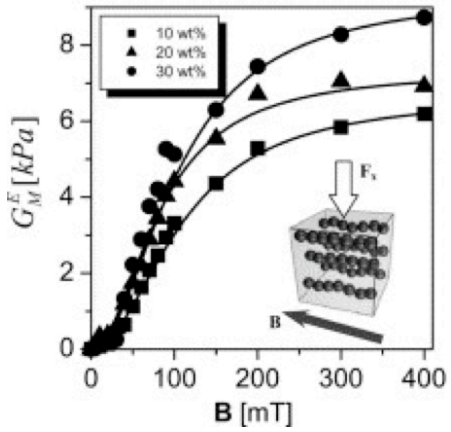

Figure 18.8: The magnetically induced excess in the modulus as a function of the applied field for several uniaxial iron-loaded PDMS elastomers. The solid lines are fits to Equation 18.2. The symbols indicate the concentration in iron particles. (Reprinted from Varga, Z., Filipcsei, G., and Zrinyi, M., *Polymer*, 46, 7779, 2005. Copyright 2005, with permission from Elsevier.)

of formation of the gel and to determine its frequency-response in a wide frequency range. Both pieces of information are essential to optimize uniaxial magnetic gels for possible applications. Before discussing the experimental results, we first recall the expectations for the sol-gel transition, and the essential features of the piezorheometer.

18.2.3.2 The sol-gel transition

Since the sol-gel transition is a connectivity transition, rheological experiments are one of the most power tools to determine the behavior of a gelling system. Here we briefly recall the changes in behavior of the complex shear modulus $G = G' + iG''$, which occur when the system evolves from the sol phase to the gel phase.

At the beginning of the chemical reaction, in the sol phase, the low frequency response of the system is liquid-like with

$$G' = \omega^2 \eta \tau \tag{18.3}$$

$$G'' = \omega \eta \tag{18.4}$$

where ω is the angular frequency, η the viscosity, and τ a relaxation time. Equations 18.3-18.4 are valid for $\omega\tau \ll 1$ (hydrodynamic regime). During the gelation process, the number and size of the polymer clusters increase leading to an increase in η and τ. At the gel point, a first cluster extends across the entire sample. The steady-shear viscosity diverges to infinity, and the equilibrium modulus starts to rise to a finite value. Beyond the gel point the low frequency response of the system is solid-type with

$$G' = G_P \tag{18.5}$$

$$G'' = \omega \eta \tag{18.6}$$

where G_P is a constant plateau value. In the gel phase, the network structure coexists with the remaining clusters which do not yet extend across the sample. The size distribution of these clusters can be deduced from the high frequency behavior of G' and G'', which is given by the following power-law

$$G' \sim G'' \sim \omega^n \tag{18.7}$$

The low frequency elastic response (i.e. G_P) of the gel continues to increase steadily until the chemical reaction is completed.

18.2.3.3 The piezorheometer

The measurements of the complex shear modulus $G = G' + iG''$ as a function of frequency were taken with the piezo-rheometer used for studying different aspects of the shear mechanical properties of elastomers [52–59], polymers [60–62] and polyelectrolyte films [63]. As schematically shown in Figure 18.9, the piezorheometer is a plate-plate rheometer that uses piezoelectric ceramics vibrating in the shear mode to apply a small strain ε to the sample and to measure the amplitude and the phase φ of the shear stress σ transmitted through the sample. The complex shear modulus of the sample is given by the stress-strain ratio $G = \sigma/\varepsilon$. It

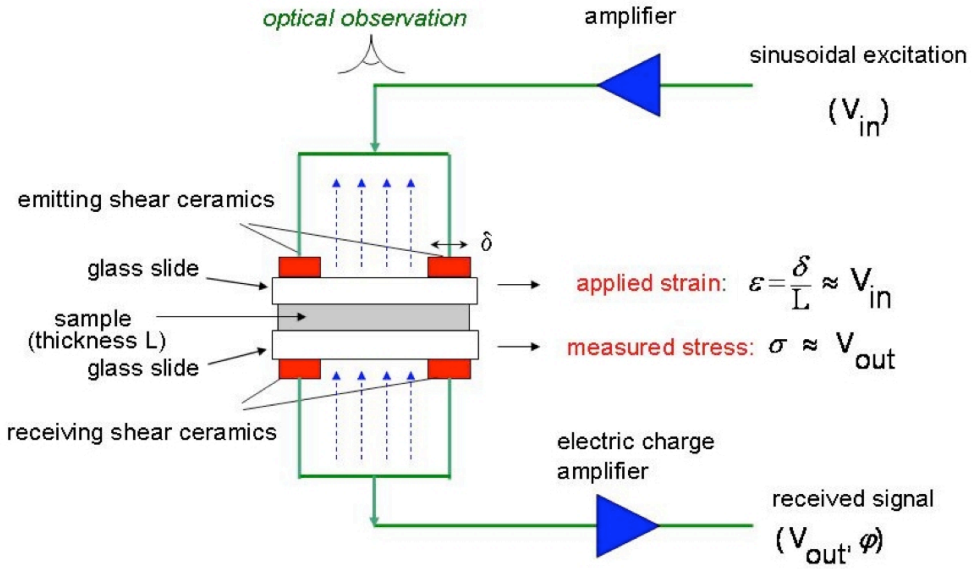

Figure 18.9: Schematic representation of the shear piezorheometer.

can be determined for sample thicknesses ranging from 10 μm to 100 μm (for viscous liquids), over a wide frequency range (10^{-2} - 10^4 Hz) and by applying very weak strains (10^{-5} - 10^{-2}). The sample has an elastic response when the strain and the stress are in-phase ($\varphi = 0$), and a viscous response when the strain and the stress have a phase difference φ of 90°. For a viscoelastic sample, the phase difference φ is in between 0° and 90°. In practice, the sample is placed between two silica slides, respectively stuck to the emitting and to the receiving ceramics. The reliability of the set-up was verified with liquids and soft solids (elastomers and gels), whose rheological properties are well known.

In the experiments presented here, G was determined for frequencies ranging from 0.2 Hz to 10^3 Hz. The applied strain ε was very small, $\sim 10^{-4}$, and the validity of the linear response was checked experimentally. Because of its small size, the cell was placed between the poles of an electromagnet during the growth of the gel and, once the gel was formed, under the objective of an optical microscope to check the organization of the magnetic particles. The experiments were performed with a homogeneous magnetic field (up to $\sim$ 1 T) applied within the plane of the sample, in a direction parallel or perpendicular to the shear direction. Additional measurements were also taken without the magnetic field. All the experiments were performed at room temperature. The samples were films with $\sim 35\mu m$ thickness and $\sim 2.5cm^2$ surface area. A PC monitoring the measuring system allowed the measurements to be carried out automatically.

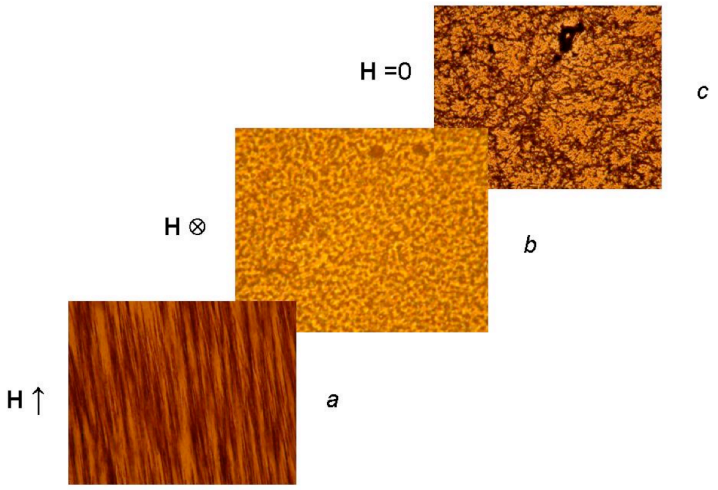

Figure 18.10: Observation under the optical microscope of the texture of a ferrogel film formed in the presence (a, b) or in the absence (c) of a magnetic field. The magnetic field is applied in a direction parallel (a) or perpendicular (b) to the plane of the sample. Size of the pictures: $170\mu m \times 130\mu m$. (Collin, D. et al. *Macromol. Rapid Commun.*, 24, 737, 2003. CopyrightWiley-VCHVerlag GmbH&Co. KGaA. Reproduced with permission.)

18.2.3.4 Results

The system studied was a magnetic PVA hydrogel filled with ferrofluid particles [38].

18.2.3.4.1 Preparation and magnetic properties of the gel

These gels were prepared by introducing a magnetic fluid (M-300 iron oxide suspension from Sigma-Hi-Chemical, Japan) into a 7.5 wt.% aqueous solution of poly (vinyl alcohol) (degree of hydrolyzation of 98-99%, M_w = 31000-50000 g/mol, from Aldrich Chemical Company). The crosslinking reaction was performed with glutardialdehyde (50 wt.% aqueous solution from Aldrich) at a pH of 1.5 (through addition of HCl 37% from Riedel-de Haën). The formation process of the magnetic gel (hereafter called ferrogel) is related to the competition between two antagonistic mechanisms associated with the fact that the ferrofluid has a pH of ~ 8, and that the cross linker does not react above pH ~ 2. Consequently, the lowering of the pH, which is necessary for the reticulation of the gel, induces a destabilization of the ferrofluid, leading to the formation of clusters of magnetic particles. This effect is compensated by the reticulation effect, which blocks the size of the clusters and their orientation in the direction of the magnetic field. As a result, the gel presents oriented fibers (length: several tens of microns, diameter: a few microns) perfectly visible with the optical microscope, as shows in Figure 18.10. For detail about the preparation of the sample see [38].

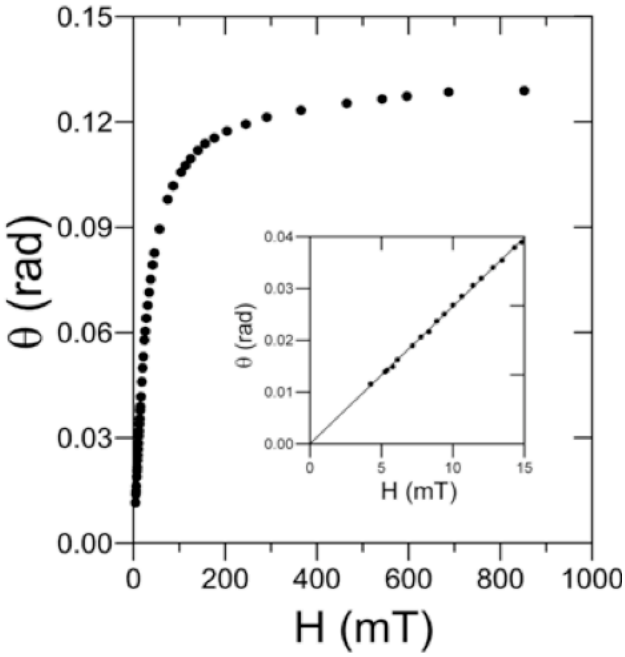

Figure 18.11: The rotation angle of a gel cylinder as a function of the magnetic field strength. The inset shows that the rotation angle is proportional to the field for small fields. (Collin, D. et al. *Macromol. Rapid Commun.*, 24, 737, 2003. CopyrightWiley-VCHVerlag GmbH&Co. KGaA. Reproduced with permission.)

To gain insight into the magnetic nature of the gel, the orientation of a cylindrical gel (the analogue of the planar sample studied in the piezorheometer) was studied as a function of the field amplitude. To do that, the gel was suspended in a homogenous magnetic field using a nonmagnetic wire of known torsional modulus. The rotation angle of the sample was then measured as a function of the field amplitude. The rotation angle is expected to be linear (ferromagnetic-like) or quadratic (paramagnetic-like) in the applied field strength. The data in Figure 18.11 show that the gel presents a ferromagnetic type response for weak fields, and that a paramagnetic contribution becomes dominant at larger fields, leading to substantial deviations from a linear law. This ferrogel is uniaxial because it can be oriented in a uniform magnetic field. Its axis of magnetization is defined by the direction of the magnetic field imposed during the reticulation.

18.2.3.4.2 Dynamical shear properties of the gel

We start with the mechanical properties of the pure PVA gel. Its formation is illustrated by Figure 18.12a, which shows the variation of G' as a function of time. The plotted values of G' correspond to the hydrodynamic behavior characterized by the frequency-independent

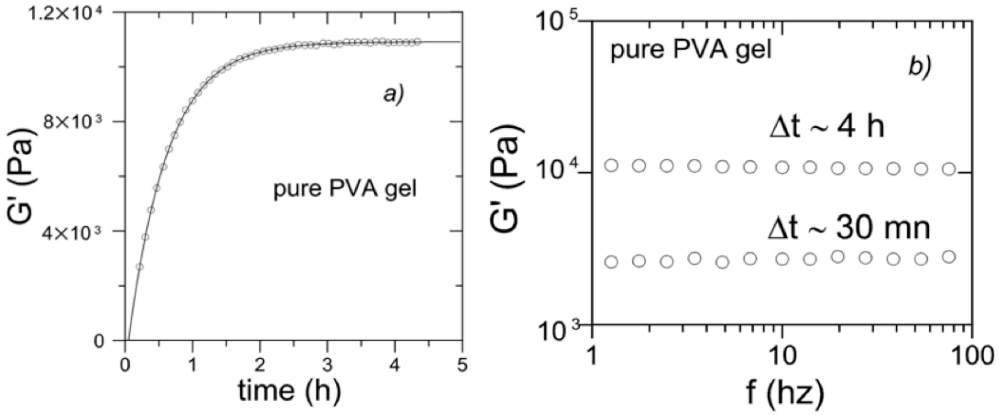

Figure 18.12: Left: variation of G' as a function of time, for a pure PVA gel. Right: frequency-dependence of G' for the same gel.

behavior of G' shown on Figure 18.12b. The solid line on Figure 18.12a shows that the fit with a stretched exponential gives a good representation of the data. The stretched exponential is given by

$$\frac{G'}{G'_\infty} = 1 - \exp\Big(-[\frac{t-t_0}{\tau}]^x\Big) \tag{18.8}$$

It contains four fit parameters. The value G'_∞ of G' for long times, the time t_0 associated with the infinite cluster, the formation time τ of the network and the exponent x describing how stretched is the exponential. The resulting parameters are $G'_\infty = (1.091 \pm 0.001) \times 10^4$ Pa, $t_0 = 0.050 \pm 0.006$ h, $x = 1.00 \pm 0.01$ and $\tau = 0.585 \pm 0.007$ h.

A typical example showing the formation of a uniaxial ferrogel in a homogeneous field is given by Figure 18.13. The data correspond to the case where $\mathbf{H}$ is parallel to $\mathbf{v}$. The field strength was 200 mT. The comparison with the time-axis of Figure 18.12a immediately shows that the presence of magnetic particles slows down considerably the kinetics of formation of the gel.

As for the pure PVA gel, Equation 18.8 provides a good fit (solid line) to the experimental data with the following parameters, $G'_\infty = (1.261 \pm 0.002) \times 10^4$ Pa, $t_0 = 1.12 \pm 0.08$ h, $x = 1.01 \pm 0.01$ and $\tau = 16.87 \pm 0.10$ h. The inset of Figure 18.13 shows that G' is frequency independent at low frequencies, indicating that the data are in the hydrodynamic regime. Similar results were obtained for $\mathbf{H}$ perpendicular to $\mathbf{v}$. However, it was not possible to determine whether the mechanical response of the gel is anisotropic or not, because the final value of G' is very sensitive to slight differences in the concentration of the ingredients (glutardialdehyde and HCl) which are involved in the preparation of the gel. In any case, the anisotropy, if it exists, is very small. This indicates that the fibers seen in Figure 18.10 are not compact objects, but rather loosely packed objects.

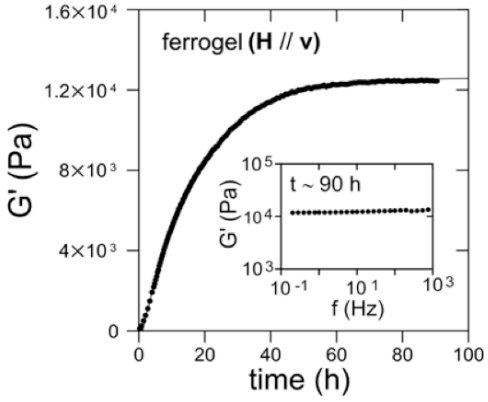

Figure 18.13: Variation of G' as a function of time for the uniaxial magnetic PVA hydrogel in the parallel orientation. A 200 mT uniform magnetic field was applied during the formation of the sample. The solid line is the fit with Equation 18.8. Inset: G' as a function of frequency at t $\sim$ 90 h. (Collin, D. et al. *Macromol. Rapid Commun.*, 24, 737, 2003. CopyrightWiley-VCHVerlag GmbH&Co. KGaA. Reproduced with permission.)

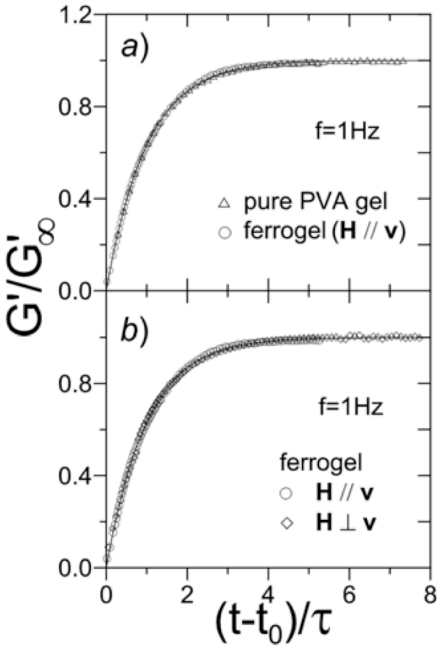

Figure 18.14: Master curves for the pure PVA gel and the uniaxial magnetic PVA gel, a) in the parallel geometry, b) for the uniaxial magnetic PVA gel in the parallel and perpendicular geometries. (Collin, D. et al. *Macromol. Rapid Commun.*, 24, 737, 2003. CopyrightWiley-VCHVerlag GmbH&Co. KGaA. Reproduced with permission.)

As shown in Figure 18.14a, a quantitative comparison between the data obtained for the pure PVA gel and for the ferrogel can be done by plotting the data for both gels as a function of the reduced variables G'/G'_∞ and $(t - t_0)/\tau$. It can be seen that both curves perfectly superimpose, giving rise to a master curve, although the τ values differ by more than one order of magnitude.

Figure 18.14b shows a similar plot for the ferrogel data associated with the parallel and perpendicular geometries. Again all the data fall on the same master curve. For all the samples, the exponent x remains around 1, indicating that these gels are characterized by a single time scale. The gel formation phenomenon is thus controlled by the same physics, regardless of whether the system is filled with magnetic particles or not.

Similar experiments are in progress on different systems for which the final material should show (or shows) a mechanical anisotropy. Also, experiments performed in the sol phase, similar to those reported in [45], should be interesting to give information about the precise nature of the interaction between the magnetic particles and the polymer network.

18.3 MACROSCOPIC STATIC AND DYNAMIC PROPERTIES

18.3.1 STATICS AND THERMODYNAMICS

18.3.1.1 Isotropic ferrogels

The macroscopic description of a system starts with the identification of the relevant variables. Apart from the quantities that are related to local conservation laws, such as mass density ρ, momentum density $\boldsymbol{g}$, energy density ε, and concentration c of the swelling fluid, we consider the elastic strain u_{ij} and the magnetization $\boldsymbol{M}$ as additional variables. In a crystal the former is related to the broken translational symmetry due the long range positional order, which gives rise to the displacement vector $\vec{u}$ as a hydrodynamic symmetry variable. Since neither solid body translations nor rigid rotations give rise to elastic deformations, the strain tensor is used as a variable, which reads in linearized version $u_{ij} = \frac{1}{2}\left(\nabla_i u_j + \nabla_j u_i\right)$. In amorphous solids, such as rubbers, gels, etc., linear elasticity is still described by a second-rank, symmetric strain tensor. For a proper description of nonlinear elasticity cf. [64]. The induced magnetization $\boldsymbol{M}$ is a slowly relaxing variable in the superparamagnetic (isotropic) case.

Assuming local thermodynamic equilibrium, i.e. all microscopic, fast relaxing quantities are already in equilibrium, we have the Gibbs relation

$$d\varepsilon = Td\sigma + \mu d\rho + \mu_c dc + v_i dg_i + H_i dB_i + h_i^M dM_i + \Psi_{ij} du_{ij}, \qquad (18.9)$$

relating all macroscopically relevant variables discussed above to the entropy density σ. $\boldsymbol{B}$ is the magnetic induction field included here in order to accommodate the static Maxwell equations. In Equation 18.9 the thermodynamic quantities, chemical potential μ, temperature T, relative chemical potential μ_c, velocity v_i, elastic stress Ψ_{ij}, magnetic field H_i, and the magnetic molecular field h_i^M, are defined as partial derivatives of the energy density with respect to the appropriate variables [50].

To determine the thermodynamic conjugate variables we need an expression for the local energy density. This energy density must be invariant under time reversal as well as under parity and it must be invariant under rigid rotations, rigid translations, and be covariant under Galilei transformations. In addition to that this energy density must have a minimum, because there exists an equilibrium state for the gel. Therefore the expression for the energy density needs to be convex. Taking into account these symmetry arguments we get [18]

$$\begin{aligned}\varepsilon = {} & \varepsilon_0 + \frac{B^2}{2} - \boldsymbol{B}\cdot\boldsymbol{M} + \frac{\mu_{ijkl}}{2}u_{ij}u_{kl} - \frac{\gamma_{ijkl}}{2}M_i M_j u_{kl} + \frac{\alpha}{2}M_i^2 + \frac{\beta}{4}\left(M_i^2\right)^2 \\ & + u_{ii}\left(\chi^\rho \delta\rho + \chi^\sigma \delta\sigma + \chi^c \delta c\right), \end{aligned} \qquad (18.10)$$

where ε_0 is the energy density of a fluid binary mixture. Equation 18.10 explicitly contains the elastic and the magnetic energy, their cross coupling (the magnetoelastic energy) and bilinear couplings of compression with the scalar variables. To discuss large elastic deformations (rubber elasticity) one should keep terms of higher order of u_{ij}, which are neglected here.

This Section is based on Refs. [18] and [47].

The magnetostrictive coupling ($\sim \gamma_{ijkl}$) is cubic [65] and the M^4 contribution is kept in order to guarantee the thermodynamic stability. The elastic tensor μ_{ijkl} (and similarly γ_{ijkl}) takes the isotropic form $\mu_{ijkl} = \mu_1\delta_{ij}\delta_{kl} + \mu_2\left(\delta_{ik}\delta_{jl} + \delta_{il}\delta_{jk} - \frac{2}{3}\delta_{ij}\delta_{kl}\right)$, where μ_1 is the compressibility and μ_2 the shear modulus. The magnetoelastic energy is similar to that for ferromagnetic materials, where, however, the compressional magnetostriction is neglected ($\gamma_1 = 0$) [65]. All static susceptibilities, such as the elastic and magnetoelastic moduli as well as those describing cross couplings between compression and the density, entropy density, and concentrations variations (χ^ρ, χ^σ, and χ^c, respectively) can depend on M^2 and are thus magnetic field strength dependent.

Using Equations 18.9 and 18.10, the magnetic Maxwell field H_i is defined in the usual way

$$H_i = \left(\frac{\partial\varepsilon}{\partial B_i}\right)_{\boldsymbol{M},u_{ij},\ldots} = B_i - M_i, \tag{18.11}$$

while the magnetic molecular field h_i^M reads

$$h_i^M = \left(\frac{\partial\varepsilon}{\partial M_i}\right)_{\boldsymbol{B},u_{ij},\ldots} = -B_i - \gamma_{ijkl}M_j u_{kl} + \alpha M_i + \beta M^2 M_i \tag{18.12}$$

Note that because of definition (Equation 18.11), it is not possible to have a direct coupling between the external field $\boldsymbol{B}$ and the strain; the deformation of the network is mediated by the magnetization via the coupling terms $\sim \gamma_{ijkl}$.

The elastic stress Ψ_{ij} has the following form

$$\Psi_{ij} = \left(\frac{\partial\varepsilon}{\partial u_{ij}}\right)_{\boldsymbol{M},\boldsymbol{B},\ldots} = \mu_{ijkl}u_{kl} - \frac{\gamma_{ijkl}}{2}M_k M_l + \delta_{ij}\left(\chi^\rho\delta\rho + \chi^\sigma\delta\sigma + \chi^c\delta c\right) \tag{18.13}$$

and depends on the magnetization.

18.3.1.2 Uniaxial ferrogels

In uniaxial ferrogels there is a permanent magnetization, which defines a preferred direction and constitutes a spontaneously broken rotational symmetry. We will introduce a unit vector m_i defined by $m_i = M_i/|\mathbf{M}|$ pointing to the direction of magnetization in analogy to the director n_i in nematic liquid crystals. But there is a significant difference. While both are even under parity, the unit vector of magnetization $\mathbf{m}$ is odd under time reversal. This will permit static as well as dynamic couplings to other variables that are odd under time reversal. We can then define the transverse Kronecker tensor $\delta_{ij}^\perp = \delta_{ij} - m_i m_j$ and we have, together with the Levi-Cevità symbol ϵ_{ijk}, three invariants of the system, by which all the static material tensors (e.g. the elastic and the magnetostrictive tensor) and the transport tensors get their uniaxial form [47]. Rotations of $\boldsymbol{M}$ are hydrodynamic excitations of the system and, therefore, the energy density should be a function of gradients of $\boldsymbol{M}$, too. This involves replacing $h_i^M dM_i$ in the Gibbs relation Equation 18.9 by $h_i^{'M}dM_i + \Phi_{ij}^M d(\nabla_j M_i)$ or using $h_i^M \equiv h_i^{'M} - \nabla_j\Phi_{ij}^M$. In addition, we consider a variable first introduced by de Gennes for liquid crystalline elastomers [66] called relative rotation $\tilde{\Omega}_i$. This variable belongs to the class of slowly relaxing

variables and describes the relative rotation between the polymer network and the orientation of the magnetization. It is defined linearly by $\tilde{\Omega}_i = \delta m_i - \Omega_i^{\perp} = \delta m_i - \frac{1}{2} m_j \left(\nabla_i u_j - \nabla_j u_i\right)$. Since m_i is a unit vector, $\mathbf{m} \cdot \delta\mathbf{m} = 0$. This variable is odd under time reversal and even under parity. For a general, nonlinear definition cf. [67]. This degree of freedom requires the additional contribution $W_i \, d\tilde{\Omega}_i$ in the Gibbs relation. It should be noted, however, that for materials with an almost rigid coupling between the direction of $\boldsymbol{M}$ and the elastic network, this degree of freedom is clamped and less important.

In the uniaxial case the local energy density, Equation 18.10, has to be amended by the appropriate additional contributions [47]

$$\begin{aligned} \varepsilon^{uniax} \quad = \quad & \frac{1}{2} K_{ijkl} (\nabla_i M_j)(\nabla_k M_l) + \frac{1}{2} D_1 \tilde{\Omega}_i \tilde{\Omega}_i + D_2 \left(m_j \delta_{ik}^{\perp} + m_k \delta_{ij}^{\perp} \right) \tilde{\Omega}_i u_{jk} \\ & + c_{ijk} g_i \nabla_j M_k + \sigma_{ijk}^{\sigma} (\nabla_i M_j)(\nabla_k \delta\sigma) + \sigma_{ijk}^{\rho} (\nabla_i M_j)(\nabla_k \delta\rho) \\ & + \sigma_{ijk}^{c} (\nabla_i M_j)(\nabla_k \delta c) \end{aligned} \tag{18.14}$$

containing a Frank-like magnetization-rotational energy, the relative rotations' energy and their energetic coupling to elastic shear, various couplings between magnetization rotation and density, temperature, and concentration gradients as well as the momentum density g_i. The latter coupling results in $g_i = \rho v_i - \rho c_{ijk} \nabla_j M_k$ and is similar to one of the couplings appearing in superfluid ^{3}He-A first introduced by Graham [68]. In this system one defines an axial vector $\mathbf{l}$ parallel to the direction of the net orbital momentum of the helium pairs. This vector does not commute with the total angular momentum vector and therefore this variable breaks the continuous rotational symmetry spontaneously, similarly to the magnetization in our system.

The uniaxial form of the static material tensors in Equations 18.10 and 18.14)as well as the resulting expressions for the thermodynamic conjugate fields (like h_i^M, W_i, Ψ_{ij} etc.) are listed in [47] and not repeated here.

18.3.2 DYNAMICS

To determine the dynamics of the variables we take into account that the conserved quantities obey a local conservation law while the dynamics of the other variables can be described by a simple balance equation where the counter term to the temporal change of the quantity is called a quasicurrent. As a set of dynamical equations we get [47]

$$\partial_t \rho + \nabla_i g_i = 0 \tag{18.15}$$

$$\partial_t \sigma + \nabla_i (\sigma v_i) + \nabla_i j_i^{\sigma} = \frac{R}{T} \tag{18.16}$$

$$\rho \partial_t c + \rho v_i \nabla_i c + \nabla_i j_i^{c} = 0 \tag{18.17}$$

$$\partial_t g_i + \nabla_j (v_j g_i + \delta_{ij} [p + \mathbf{B} \cdot \mathbf{H}] + \sigma_{ij}^{th} + \sigma_{ij}) = 0 \tag{18.18}$$

$$\partial_t M_i + v_j \nabla_j M_i + (\mathbf{M} \times \omega)_i + X_i = 0 \tag{18.19}$$

$$\partial_t u_{ij} + v_k \nabla_k u_{ij} + Y_{ij} = 0 \tag{18.20}$$

$$\partial_t \tilde{\Omega}_i + v_k \nabla_k \tilde{\Omega}_i + Z_i = 0 \tag{18.21}$$

where we have introduced the vorticity $\omega_i = (1/2)\epsilon_{ijk}\nabla_j v_k$ and the thermodynamic part of the stress tensor $\sigma_{ij}^{th} = -\frac{1}{2}\left(B_i H_j + B_j H_i\right) + \frac{1}{2}\left(\Psi_{jk}\epsilon_{ki} + \Psi_{ik}\epsilon_{kj}\right)$ according to the requirement that the energy density should be invariant under rigid rotations [50]. The pressure $p = \partial\left(\int \varepsilon\, dV\right)/\partial V$ in Equation 18.18 is given by $p = -\varepsilon + \mu\rho + T\sigma + \mathbf{v}\cdot\mathbf{g}$.

For practical reasons we have used an entropy balance equation 18.16 rather than the energy conservation law; both are not independent but related through the Gibbs relation (Equation 18.9). In the equation for the entropy density we introduced R, the dissipation function which represents the entropy production of the system. Due to the second law of thermodynamics R must satisfy $R \geq 0$. For reversible processes this dissipation function is equal to zero while for irreversible processes it must be positive. In the following we will split the currents and quasicurrents into reversible parts (denoted with a superscript R) and irreversible parts (denoted with a superscript D).

If we again make use of the symmetry arguments mentioned above and use Onsager's relations we obtain the following expressions for the reversible currents up to linear order in the thermodynamic forces [47]

$$
\begin{aligned}
j_i^{\sigma R} &= -\kappa_{ij}^R \nabla_j T - D_{ij}^{TR}\nabla_j \mu_c + \xi_{ij}^{TR}\nabla_l \Psi_{jl} && (18.22)\\
j_i^{cR} &= -D_{ij}^R \nabla_j \mu_c + D_{ij}^{TR}\nabla_j T + \xi_{ij}^{cR}\nabla_l \Psi_{lj} && (18.23)\\
\sigma_{ij}^R &= -\Psi_{ij} - c_{ijk}^{RJ} h_k^M - \nu_{ijkl}^R A_{kl} + \xi_{ijk}^{\sigma R} W_k && (18.24)\\
Y_{ij}^R &= -A_{ij} + \xi_{ijk}^{YR} W_k + \frac{1}{2}\lambda^M \left[\nabla_i (\nabla \times \mathbf{h}^M)_j + \nabla_j (\nabla \times \mathbf{h}^M)_i\right] \\
&\quad -\frac{1}{2}\nabla_i (\xi_{jk}^R \nabla_l \Psi_{kl} + \xi_{jk}^{TR}\nabla_k T + \xi_{jk}^{cR}\nabla_k \mu_c) \\
&\quad -\frac{1}{2}\nabla_j (\xi_{ik}^R \nabla_l \Psi_{kl} + \xi_{ik}^{TR}\nabla_k T + \xi_{ik}^{cR}\nabla_k \mu_c) && (18.25)\\
X_i^R &= b_{ij}^R h_j^M + \lambda^M \epsilon_{ijk}\nabla_j \nabla_l \Psi_{kl} - c_{jki}^{RJ} A_{jk} + \xi_{ij}^{XR} W_j && (18.26)\\
Z_i^R &= \tau_{ij}^R W_j - \xi_{ij}^{XR} h_j^M - \xi_{kli}^{\sigma R} A_{kl} - \xi_{kli}^{YR}\Psi_{kl} && (18.27)
\end{aligned}
$$

In isotropic ferrogels the quasicurrent Z_i^R is absent as well as the appropriate counter terms $\sim \xi_{ij}^{XR}$, $\xi_{kli}^{\sigma R}$, and ξ_{kli}^{YR} in X_i^R, σ_{ij}^R, and Y_{ij}^R, respectively. These terms describe the reversible dynamic coupling of relative rotations to the magnetization, the momentum density and the network. The first coupling – mediated by the tensor ξ_{ij}^{XR} – is a new term that exists neither in nematic liquid crystalline elastomers [69] nor in superfluid ^{3}He-A, while the second coupling, $\xi_{ijk}^{\sigma R}$, already appeared in superfluid ^{3}He-A and the third one, ξ_{ijk}^{YR}, in nematic liquid crystalline elastomers.

All the second rank tensors have to be odd under time reversal and are of the form $\alpha_{ij}^R = \alpha^R \epsilon_{ijk}\, m_k$ resembling the form of a Hall conductance. In the isotropic case, m_i has to be replaced by the induced magnetization or by the external field. These reversible linear field contributions to transport parameters or tensors are known even for isotropic fluids (κ^R, Righi-Leduc effect) and some of them have been discussed in detail for ferronematics [70] and isotropic ferrofluids [71]. the third and fourth rank material tensors are listed in [18, 47]. Again, for isotropic ferrogels these reversible couplings are absent, if there is no external magnetic field.

We can use the dissipation function R as a Liapunov functional to derive the irreversible currents and quasicurrents. One can expand the function R (R/T is the amount of entropy produced within a unit volume per unit time) into the thermodynamic forces using the same symmetry arguments as in the case of the energy density. We obtain [47]

$$\begin{aligned} R &= \frac{1}{2}\kappa_{ij}(\nabla_i T)(\nabla_j T) + D^T_{ij}(\nabla_i T)(\nabla_j \mu_c) + \xi^T_{ij}(\nabla_i T)(\nabla_k \Psi_{jk}) + \frac{1}{2}\nu_{ijkl}A_{ij}A_{kl} \\ &+\frac{1}{2}D_{ij}(\nabla_i \mu_c)(\nabla_j \mu_c) + \xi^c_{ij}(\nabla_i \mu_c)(\nabla_k \Psi_{jk}) + \frac{1}{2}\xi_{ij}(\nabla_k \Psi_{ik})(\nabla_l \Psi_{jl}) \\ &+\xi^\sigma_{ijk}A_{ij}W_k + c^J_{ijk}A_{ij}h^M_k + \frac{1}{2}b_{ij}h^M_i h^M_j + \frac{1}{2}\tau W_i W_i + \xi^X W_i h^M_i \end{aligned} \tag{18.28}$$

where we have introduced various second rank dissipative transport tensors describing heat conduction (κ), diffusion (D) and thermo-diffusion (D^T) , elastic (or vacancy) diffusion (ξ) and appropriate cross couplings to temperature (ξ^T) and concentration gradients (ξ^c) , and magnetization relaxation (b). These tensors are of the form $\alpha_{ij} = \alpha_{||} m_i m_j + \alpha_\perp \delta^\perp_{ij}$, reducing to $\alpha_{ij} = \alpha\, \delta_{ij}$ in the isotropic case. The third rank tensor $\xi^\sigma_{ijk} = \xi^\sigma\,(m_i \epsilon_{jkl} + m_j \epsilon_{ikl})\, m_l$ vanishes in the isotropic case as well as τ and ξ^X due to the lack of relative rotations. Only c^J_{ijk} can exist in isotropic ferrogels, but is proportional to the square of the external magnetic field strength. The viscosity tensor ν_{ijkl} has the standard isotropic or uniaxial form.

To obtain the dissipative parts of the currents and quasicurrents one has to take partial derivatives with respect to the appropriate thermodynamic forces, e.g. $Y^D_{ij} = \partial R/\partial \Psi_{ij}$, $Z^D_i = \partial R/\partial W_i$, or $\sigma^D_{ij} = -\partial R/\partial(\nabla_j v_i)$. Again, explicit expressions are listed in [18, 47].

18.4 EXAMPLES FOR NOVEL CROSS-COUPLING EFFECTS

18.4.1 MAGNETOSTRICTION

18.4.1.1 Static elongation and shear

For isotropic ferrogels we first discuss static elastic deformations in the presence of an external field. Magnetostriction leads to an anisotropic deformation. If then an external strain is applied, the stress-strain relation is more complicated than a simple Hooke's law.

In equilibrium, both the elastic stress Equation 18.13 and the magnetic molecular field Equation18.12 have to be zero. Without an external field or external strain there is no magnetization and no strain in equilibrium. A finite external field, taken along the z axis, $\boldsymbol{B} = B_0 \boldsymbol{e}_z$, induces an equilibrium magnetization ($\boldsymbol{M}^0 = M_0 \boldsymbol{e}_z$) and a nonzero strain u^0_{ij} due to the magnetostriction effect. Neglecting the couplings of density, entropy, and concentration to the strain tensor, we have [18]

$$u^0_{xx} = u^0_{yy} = \frac{\mu_2\gamma_1 - \mu_1\gamma_2}{6\mu_1\mu_2} M_0^2, \tag{18.29}$$

$$u^0_{zz} = \frac{\mu_2\gamma_1 + 2\mu_1\gamma_2}{6\mu_1\mu_2} M_0^2, \tag{18.30}$$

This Section is based on Refs. [18], [47], [48], and [49].

leading to the volume change $U^0 \equiv u^0_{xx} + u^0_{yy} + u^0_{zz} = (\gamma_1/2\mu_1)M_0^2$. The magnetostrictive volume change of the ferrogel is determined by the bulk modulus μ_1 and by the coefficient γ_1, which couples the trace of the stress tensor to the magnitude of the magnetization.

Magnetostriction is a well-known phenomenon in single- or polycrystalline ferromagnetic solids [72]. Ferrogels are isotropic and nonmagnetic without an external magnetic field and magnetostriction is then a nonlinear effect. The induced deformations, Equations 18.29 and 18.30, are of uniaxial symmetry and in this state the ferrogel behaves more like a uniaxial ferromagnet than an isotropic one.

This state is then disturbed by an external deformation Δu_{ij} by some mechanical device. Due to the magnetostriction effect this gives also rise to a change in the magnetization. In the static limit the magnetic degree of freedom is still in equilibrium and the change of the magnetization can be obtained from the condition $h_i^M = 0$, Equation 18.12. The applied deformations give, directly by Hooke's law, and indirectly by the change of the magnetization, elastic stresses [18]

$$\begin{aligned}
\Psi_{zz} &= (\mu'' - \chi_0\gamma''^2 M_0^2)\Delta u_{zz} + (\mu' - \chi_0\gamma'\gamma'' M_0^2)(\Delta u_{xx} + \Delta u_{yy}), && (18.31)\\
\Psi_{xx} &= (\mu'' - \chi_0\gamma'^2 M_0^2)\Delta u_{xx} + (\mu' - \chi_0\gamma'^2 M_0^2)\Delta u_{yy} \\
&\quad +(\mu' - \chi_0\gamma'\gamma'' M_0^2)\Delta u_{zz}, && (18.32)\\
\Psi_{zx} &= 2(\mu_2 - \chi_0\gamma_2^2 M_0^2)\Delta u_{zx}, && (18.33)\\
\Psi_{xy} &= 2\mu_2 \Delta u_{xy} && (18.34)
\end{aligned}$$

with two additional relations similar to Equations 18.32,18.33, but with x and y subscripts interchanged. For the magnetic susceptibility, $\chi_0 = \chi(B_0)$, its value at the external field strength B_0 has to be taken while $\mu'' = \mu_1 + (4/3)\mu_2$ and $\mu' = \mu_1 - (2/3)\mu_2$ and similar abbreviations for the $\gamma's$ are used. Note that, even if the deformation does conserve the volume ($\Delta u_{xx} + \Delta u_{yy} + \Delta u_{zz} = 0$), the trace of the elastic stress tensor is not zero, but given by $\Psi_{kk} = -6\chi_0\gamma_1\gamma_2 M_0^2 \Delta u_{zz}$. Formulas 18.31–18.34 are applicable for small strains only, since it is based on Hooke's law, while for larger strains deviations from this law due to rubber elasticity are to be expected.

The effective elastic moduli, i.e. the ratio between the measured stress and the applied strain, e.g. $\Psi_{zz}/\Delta u_{zz}$ or $\Psi_x/\Delta u_x$, show a decrease as a function of the applied field due to magnetostriction. This is in contrast to the experiments shown in Figure 18.8, where an increase is found. Thus, for the materials discussed in Figure 18.8 magnetostriction is a small effect, completely dominated by the intrinsic field dependence of the material parameters, $\mu''(M_0) - \mu'' \sim M_0^2$. The latter effect is non-hydrodynamic and based on microscopic structure changes due to the external field. The proportionality factor can be obtained from experiments and is positive for the materials discussed here.

18.4.1.2 Propagation of sound

Due to the presence of the permanent polymer network in ferrogels compared to ferrofluids, there are transverse as well as longitudinal sound eigenmodes. In this Section we derive the longitudinal and the transverse sound of the system with an external magnetic field parallel to the z axis. We neglect all diffusional processes connected, e.g., with viscosity and heat

conduction as well as their reversible counterparts. Only the relaxation of the magnetization field is kept.

Assuming a one-dimensional plane wave with space-time dependence $\sim \exp i(-\omega t + \boldsymbol{k}\cdot\boldsymbol{r})$ for all deviations δu_{ij}, δM_i, v_i, $\delta\rho$ from the equilibrium values, the linearized set of dynamic equations becomes an algebraic one. We consider sound in the two cases, where the external magnetic field and the equilibrium magnetization are either perpendicular or parallel to the wave vector. Field fluctuations δB_i are fixed by the static Maxwell equations to $\delta B_i = \delta M_j(\delta_{ij} - k_i k_j k^{-2})$.

In the low frequency limit ($\omega < 1/\tau_M$) below the magnetization relaxation frequency and for the external field being perpendicular to the wave vector the velocities of the longitudinal c_l and the transverse sounds c_{t1}, c_{t2} read [18]

$$c_l^2 = \frac{\tilde{\mu}(M_0)}{\rho} - \tilde{\mu}\,\frac{\mu_2\gamma_1 - \mu_1\gamma_2}{6\rho\mu_2\mu_1}\,M_0^2, \tag{18.35}$$

$$c_{t1}^2 = \frac{\mu_2(M_0)}{\rho} - \frac{\mu_2\gamma_1 - \mu_1\gamma_2}{6\rho\mu_1}M_0^2, \tag{18.36}$$

$$c_{t2}^2 = \frac{\mu_2(M_0)}{\rho} - \frac{2\mu_2\gamma_1 + 7\mu_1\gamma_2}{12\rho\mu_1}\,M_0^2, \tag{18.37}$$

while for a parallel field the transverse sound velocities are equal according to the effectively uniaxial symmetry due to the external field.

The sound speeds at low frequencies and zero field give information about the compressibility and the elastic moduli (bulk and shear). There is a dependence on M_0^2 due to intrinsic field dependence of the moduli as measured by static experiments. However, even if the static magnetostrictive effect is neglected (as done in Equations 18.35-18.37), there are additional contributions $\sim M_0^2$. They are of the bilinear $\gamma\mu$ type and a dynamic manifestation of magnetostriction emerging through the nonlinear elastic stress contribution to the stress tensor in σ_{ij}^{th}, which, however, is effectively linear due to the non-zero equilibrium strains. Therefore, the effective moduli measured by sound propagation in an external field are different from those given by the static elastic stress Ψ_{ij} discussed in the preceding Section. The coincidence of static linear elasticity and low frequency sound speed is restored in the limit of vanishing magnetic field, when no magnetostrictive deformation is present and the additional contribution in the stress tensor σ_{ij}^{th} is nonlinear and absent in the sound spectra. Of course, in this limit the sound spectra are isotropic as is the ferrogel.

The sound velocities change with an external magnetic field basically with the second power of the field, which is in accordance with experiments on longitudinal sound [10]. Whether the sound velocities are decreased or increased by the field cannot be established by general rules, since the signs of $\gamma_{1,2}$ are not fixed and can be material dependent. Measurements of transverse and longitudinal sound velocities in the different geometries will provide information on the magnitude and sign of the magnetostrictive and elastic moduli. As a first approximation the magnetostrictive volume change ($\sim \gamma_1 M_0^2/\mu_1$) can be neglected in those rubbers and only shape changes remain.

Damping of sound waves generally is rather weak and given by the imaginary part of the dispersion relation. In addition to the usual magnetic-field-independent sound damping

due to viscosity and other diffusional processes there is a field-dependent sound damping in ferrogels. This is an effect of the reversible, dynamic coupling of the magnetization to flow, either phenomenological [$c^R_{ijk}(M)$ in Equation 18.26] or kinematic [$\epsilon_{ijk}M_j\omega_k$ in Equation 18.19] and its counterparts in the Navier-Stokes equation. For example, when the magnetic field is parallel (perpendicular) to the wave vector a field-dependent damping of longitudinal (transverse) sound reads, respectively, [18]

$$\mathfrak{Im}(\omega_l) = -\frac{1}{2}\frac{\left[\chi_0\gamma'' - \left(2c_1^R + c_2^R\right)\right]^2}{\rho b}M_0^2k^2, \tag{18.38}$$

$$\mathfrak{Im}(\omega_{t2}) = -\frac{1}{2}\frac{\left(\chi_0\gamma_2 - c_1^R + \frac{1}{2}\right)^2}{\rho b}M_0^2k^2, \tag{18.39}$$

the first of which can be related to the observed increase of the apparent viscosity due to the magnetic field [73]. In all cases $\mathfrak{Im} < 0$, as it should be according to the second law of thermodynamics.

We will not investigate the high frequency limit for $\omega > 1/\tau_M$, since for higher frequencies possible viscoelastic effects should also be taken into account, which goes beyond the scope of this review.

18.4.2 SHEAR INDUCED MAGNETIZATION

Uniaxial ferrogels differ qualitatively from the isotropic ones by the macroscopic variables associated with relative rotations. These variables describe, as already mentioned, the relative rotations between the orientation of the magnetization and the polymer network. In this Section we discuss an effect associated with these variables. We apply a constant shear flow and determine the change of magnetization. We assume that the direction of the permanent magnetization of the uniaxial ferrogel $\boldsymbol{m} = \boldsymbol{e}_x$ is parallel to the flow direction of an external stationary shear flow $S_{kl} = S^{ext}\delta_{ky}\delta_{lx}\nabla_k v_l$. Furthermore we assume spatial homogeneity and consider only linear effects. Contributions due to magnetostriction effects are neglected. We do not apply an external magnetic field. Therefore we can assume that the magnitude of the magnetization is not changed but only its direction $\boldsymbol{M} = M_0\left(\boldsymbol{m} + \delta\boldsymbol{m}\right)$.

The resulting set of inhomogeneous algebraic equations for the four variables δm_y, δm_z, u_{xy}, and u_{xz} has the following solutions [47]

$$\delta m_y = \frac{b^R(\xi^X + 2\xi^{YR}c^J) - b_\perp(\xi^{XR} - 2\xi^{YR}c_1^{RJ})}{2\xi^{YR}(\alpha M_0 - B_0)(b_\perp^2 + b^{R2})}S^{ext} \tag{18.40}$$

$$\delta m_z = -\frac{b_\perp(\xi^X + 2\xi^{YR}c^J) + b^R(\xi^{XR} - 2\xi^{YR}c_1^{RJ})}{2\xi^{YR}(\alpha M_0 - B_0)(b_\perp^2 + b^{R2})}S^{ext} \tag{18.41}$$

For this experimental setup we thus predict a rotation of the magnetization within the shear plane, $\delta m_y \neq 0$, as well as out of the shear plane, $\delta m_z \neq 0$, which are both proportional to the applied external force. This effect is due to the variables associated with relative rotations, because all contributions are proportional to either ξ^{XR}, ξ^X, or ξ^{YR}, which represent the (reversible) dynamical coupling of relative rotations to the magnetization and the strain

field, respectively. Reversible (superscript R) and irreversible transport parameters are systematically paired in the numerator. There are elastic deformations as well, not only in the shear plane, but also out of the shear plane, u_{xz}, which are constant and proportional to S^{ext}. For oscillatory shear $S^{ext} \rightarrow S^{ext} exp(i\omega t)$ the same variables as in the static case will be excited with the same frequency, but will show some phase lag due to various dissipation effects. The change of the direction of the magnetization obtained should be observable by Hall probes, if the degree of freedom of relative rotations is operable and not clamped in the ferrogel used.

18.4.3 SURFACE WAVES AND ROSENSWEIG INSTABILITY

18.4.3.1 Surface waves in isotropic ferrogels

Surface undulations of the free surface of viscous liquids are known to be able to propagate as gravity or capillary waves. In more complex systems like viscoelastic liquids or gels the transient or permanent elasticity allows for modified transverse elastic waves at free surfaces [74]. They are excited e.g. by thermal fluctuations or by imposed temperature patterns on the surface. In ferrofluids magnetic stresses at the surface come into play. In particular, in an external magnetic field normal to the surface there is a focusing effect on the magnetization at the wave crests of an undulating surface with the tendency to increase the undulations [75]. At a critical field strength no wave propagation is possible and the surface becomes unstable with respect to a stationary pattern of surface spikes (Rosensweig or normal field instability). Combining the two aspects of elasticity and superparamagnetic response and using linearized dynamic equations and boundary conditions we get the general surface wave dispersion relation for ferrogels (in a normal external field), which contains as special cases those for ferrofluids and non-magnetic gels and can be generalized to viscoelastic ferrofluids and magnetorheological fluids. A linear stability analysis reveals the threshold condition, above which stationary surface spikes grow. This critical field depends on gravity, surface tension and on the elastic (shear) modulus of the gel, while the critical wavelength of the emerging spike pattern is independent of the latter. As in the case of ferrofluids neither the threshold nor the critical wavelength depends on the viscosity.

To derive the surface wave dispersion relation several approximations are made [48]. Of the various reversible and irreversible dynamic cross couplings between flow, elasticity and magnetization discussed above, we only keep those of them, which are presumably the relevant ones for the present problem. In particular, we keep the magnetic Maxwell and the elastic and viscous contributions to the stress tensor. The magnetization $\boldsymbol{M}$ is assumed to have relaxed to its static value given by the magnetic field and magnetostatics, $\mathrm{div}\boldsymbol{B} = 0$ and $\mathrm{curl}\boldsymbol{H} = 0$, can be applied. Global incompressibility, $\mathrm{div}\boldsymbol{v} = 0$, and incompressibility of the gel network, $u_{kk} = 0$, is employed and only the shear elastic modulus μ_2 and the shear viscosity ν_2 enter the stress tensor.

Neglecting the thermal degree of freedom, magnetostriction, and taking the simplest form

for the dynamics of the elasticity we are left with the linearized dynamic equations

$$\frac{\partial}{\partial t}\rho v_i + \nabla_j \sigma_{ij} = -\rho g \delta_{iz} \tag{18.42}$$

$$\frac{\partial}{\partial t}\epsilon_{ij} - \frac{1}{2}(\nabla_i v_j + \nabla_j v_i) = 0\,. \tag{18.43}$$

where the gravitational force ($\sim g$) is acting along the negative z axis.

We model our system by an originally flat surface $z = 0$ dividing the magnetic gel ($z < 0$) from vacuum ($z > 0$), where the applied external field ($\boldsymbol{B}^{vac} = B_0 \boldsymbol{e}_z = \boldsymbol{H}^{vac}$) is normal to the surface.

At the free surface we need boundary conditions for our dynamic variables. First, there are the magnetic ones [76], the mechanical ones guaranteeing a stress-free surface, and the (linearized) kinematic one

$$\boldsymbol{e} \times \boldsymbol{H} = \boldsymbol{e} \times \boldsymbol{H}^{vac} \qquad \boldsymbol{e} \cdot \boldsymbol{B} = \boldsymbol{e} \cdot \boldsymbol{B}^{vac} \tag{18.44}$$

$$\boldsymbol{e} \times \sigma \cdot \boldsymbol{e} = \boldsymbol{e} \times \sigma^{vac} \cdot \boldsymbol{e} \tag{18.45}$$

$$\boldsymbol{e} \cdot \sigma \cdot \boldsymbol{e} - \boldsymbol{e} \cdot \sigma^{vac} \cdot \boldsymbol{e} = \rho\, g\, \xi + \sigma\, \mathrm{div} \boldsymbol{e} \tag{18.46}$$

$$\frac{\partial}{\partial t}\xi = v_z \tag{18.47}$$

where $\xi(x, y, t)$ describes surface displacements. The unit vector $\boldsymbol{e}$ is the surface normal, $\boldsymbol{e} = \boldsymbol{\nabla}(z - \xi)/|\boldsymbol{\nabla}(z - \xi)|$, and $\mathrm{div}\boldsymbol{e}$ is twice the mean curvature. The vacuum stresses (superscript vac) are solely due to the magnetic fields (vacuum Maxwell stress tensor). The normal stress difference between the magnetic gel and the vacuum is balanced by gravity and the Laplace stress due to curvature of the surface and the surface tension σ.

The system of equations and boundary conditions 18.42-18.47 always has the trivial solution (ground state), where the surface is flat ($\xi = 0$, $\boldsymbol{e}_0 = \boldsymbol{e}_z$), flow and deformations are absent ($\boldsymbol{v} = 0$, $u_{ij} = 0$), and the fields are constant ($\boldsymbol{M}_0 = M_0 \boldsymbol{e}_z$ with $M_0 = (1 - 1/\mu)B_0$, where μ is magnetic permeability).

We now allow for periodic surface undulations $\xi(x, y, t) = \hat{\xi} \exp(-ik_x x - ik_y y + i\omega t)$ with frequency $\omega = \omega_0 - i\lambda$ (ω_0 and λ real) and wave vector $\boldsymbol{k} = (k_x, k_y, 0)$ describing propagating and damped surface waves. For $\omega = 0$ a stationary spatial pattern is obtained. Generally ω is a complex function of $\boldsymbol{k}$. Deviations from the ground state of all the other variables have to be proportional to $\xi(x, y, t)$ and in a linear theory the amplitude $\hat{\xi}$ is undetermined.

To have a nontrivial solution for the resulting set of linear algebraic equations, the determinant of coefficients must vanish. This leads to the dispersion relation of surface waves for ferrogels [48]

$$\rho\omega^2 \left(2\tilde{\mu}_2(\omega)k^2 - \rho\omega^2\right) + \rho\omega^2 \left(\sigma k^3 + \rho g k + 2\tilde{\mu}_2(\omega)k^2 - \frac{\mu}{1+\mu} M_0^2 k^2\right) - 4\tilde{\mu}_2^2(\omega)\, k^4 \left[1 - \left(1 - \frac{\rho\omega^2}{\tilde{\mu}_2(\omega)k^2}\right)^{1/2}\right] = 0\,. \tag{18.48}$$

with the frequency dependent $\tilde{\mu}_2(\omega) \equiv \mu_2 + i\omega\nu_2$. In the absence of an external magnetic field ($M_0 = 0$) Equation 18.48 reduces to the dispersion relation for nonmagnetic gels [74]. It also contains as a special case the surface wave dispersion relation for ferrofluids (in an external field) by choosing $\tilde{\mu}_2 = i\omega\nu_2$. It can be generalized to viscoelastic ferrofluids, whose elasticity relaxes on a time scale τ^{-1}, by replacing μ_2 with $i\omega\tau\mu_2/(1 + i\omega\tau)$ [74], and to magnetorheological fluids by allowing μ_2, ν_2, and τ to be functions of the external field.

18.4.3.2 Rosensweig instability

The effect of an external magnetic field perpendicular to the surface is a destabilizing one [75]. From Equation 18.48 it is evident that an external field leads to an effective reduction of the surface stiffness (provided by surface tension, gravity or elasticity) and decreases the frequency (squared) of the propagating waves in all regimes by $\sim M_0^2 k^2$. If the field is large enough, this reduction is the dominant effect and can lead to $\omega = 0$ and thus, to the breakdown of propagating waves. Indeed, Equation 18.48 can be slightly reinterpreted: It is an equation for that external field strength (or M_0), where a surface disturbance with wave vector k and frequency ω_0 relaxes to zero or grows exponentially for λ negative or positive, respectively. For $\lambda = 0$ such a surface disturbance is marginally stable (or unstable) against infinitesimal disturbances. The function M_0 still depends on ω_0 and k and has to be minimized with respect to the latter quantity in order to get the true instability threshold.

For $\omega_0 = 0$ (stationary instability) the linear threshold condition is completely independent of ν_2 and simplifies to [48]

$$M_0^2 = \frac{1+\mu}{\mu}\left(\sigma k + \frac{\rho g}{k} + 2\mu_2\right) . \tag{18.49}$$

Minimizing with respect to k leads to the critical wave vector $k_c = \sqrt{\rho g/\sigma}$ and the critical field $M_c^2 = (2/\mu)(1+\mu)\left(\sqrt{\sigma\rho g} + \mu_2\right)$. Obviously, k_c is identical to that in ferrofluids and not dependent on elasticity, but the critical field is enhanced by elasticity. The latter finding is no surprise, since elasticity increases the surface stiffness. For typical polymer gels with a shear elastic modulus of 1 kPa, the elastic contribution to M_c exceeds the surface tension contribution roughly by a factor of 5 and elasticity is the dominant factor. Critical values of 100 - 200 Gauss for M_0 have to be expected for typical samples. The critical wavelength is in the range of 1 cm, which for surface waves lies in the elasticity dominated regime. Thus, if the system cannot choose the optimal (critical) wavelength, but is fixed to a prescribed one like in many surface wave scattering experiments, the field necessary to destabilize the surface wave is about M_c in the elastic regime and higher in the other ones, where $k > k_c$ or $k < k_c$. For very soft gels with $\mu_2 < 10$ Pa, the influence of the elasticity is rather negligible and ordinary ferrofluid behavior is found.

A linear theory can neither determine the actual spike pattern, nor the true nature of the instability (forward, backward etc.). The standard weakly nonlinear (amplitude expansion) theory that provides suitable amplitude equations, by which these questions can be answered, is more complicated in the present situation due to two problems. First the driving force of the instability is manifest in the boundary conditions, but not in the bulk equations, and second the surface profile (the location where the boundary conditions have to be applied)

changes with the order of the amplitude expansion. Thus, for ferrofluids a different path has been chosen [77, 78]. Neglecting the viscosity (and all other dynamic processes) from the beginning, the system is Hamiltonian and its stability governed by a free energy, more precisely by the surface free energy, since the magnetic destabilization acts at the surface. We generalize this approach to (isotropic) ferrogels by taking into account in addition the elastic free energy [49]. The results have to be taken with the caveat that neglecting the viscosity is justified at the (linear) instability threshold, but is an unproven assumption for the nonlinear domain and for the pattern formation and selection processes.

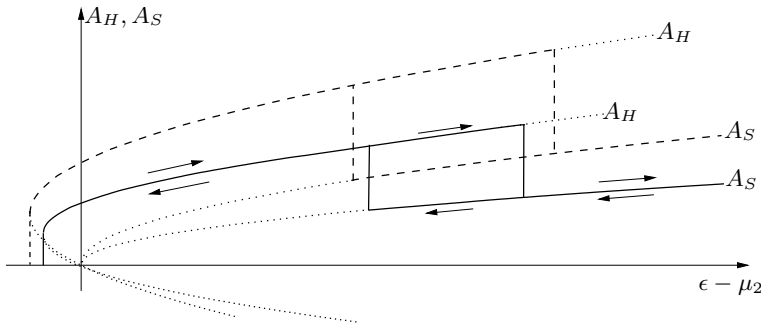

Figure 18.15: Qualitative sketch (not to scale) of the evolution of the amplitudes for squares (A_S) and hexagons (A_H) [adopted from [49] (with permission)]. The dashed lines correspond to the case of a ferrofluid while the solid lines qualitatively describe the behavior for ferrogels with finite shear modulus μ_2. The dotted lines represent the unstable branches. (Adapted from Bohlius, S., Pleiner, H., and Brand, H.R., *J. Phys. Cond. Matter*, 18, S2671, 2006.)

After some rather involved algebraic calculations the stability diagram for a square and a hexagon spike pattern is obtained (Figure 18.15) where the amplitudes are shown as function of the reduced external field strength ($\epsilon = \mu_2$ constitutes the linear threshold field). We note a decrease in size of the hysteretic region (for negative $\epsilon - \mu_2$) with increasing shear modulus. The second hysteretic region for the transition between squares and hexagons also shrinks with increasing μ_2. This result should be experimentally detectable, at least qualitatively. This picture has recently been corroborated by deriving the amplitude equation for this problem [79].

18.5 A COMPARISON WITH THE PHYSICAL PROPERTIES OF LIQUID CRYSTALLINE GELS AND ELASTOMERS

Most of the other chapters of this book deal with the preparation, the characterization and the physical properties of liquid crystalline gels and liquid crystalline elastomers (cf. [80] for an early review covering the material until about 1998). Therefore we discuss here briefly similarities and differences of these systems compared to the magnetic gels studied in this chapter.

First of all one notices a big difference in the width of the hydrodynamic regime for water-based gels like PVA gels. For example, from the completely flat plateau value of G' shown in the inset of Figure 18.13 we conclude that the hydrodynamic regime for this class of magnetic gels covers at least the frequency range from 100 mHz to 1 kHz, that is four orders of magnitude. We note that the upper bound for the frequency of the hydrodynamic regime in magnetic gels is actually not known as yet, since the technical limitation of the piezorheometer used for these experiments set an upper limit of about 2 kHz. However, clearly the upper bound must be lower than that for a water- or acetone-based magnetic fluid, which is typically about 2 MHz. In contrast to PVA gels, PDMS gels have a much reduced hydrodynamic regime and show a cross-over to non-hydrodynamic behavior around 100 Hz. This can be traced back to the viscoelastic effects of the PDMS gels.

These observations should be compared with our knowledge about the hydrodynamic regime in the fields of liquid crystalline gels and elastomers. There we have shown (cf., e.g., Ref. [57], that the cross-over from the hydrodynamic regime to the regime, where more microscopic, non-hydrodynamic effects become important, takes place at about 10 to 100 Hz for a nematic elastomer as is evidenced by the frequency dependence of G' and G''. Even earlier we have already pointed out [53, 54], that for smectic A elastomers this cross-over arises for even lower frequencies ($\sim 1 - 10$ Hz), thus cutting down even further in frequency the applicability of the hydrodynamic approach in these layered systems. In Refs. [53, 54] this further reduction of the hydrodynamic regime has been linked to the formation of giant clusters involving the mesogenic side-chains organized in layers.

From this comparison it emerges, that magnetic gels have a comparable hydrodynamic range to liquid crystalline elastomers, when they are based on typical polymers (PDMS), while there is a much larger hydrodynamic regime than in most LCEs when they are water-based like magnetic gels on PVA basis. We note that from the dynamic investigations of magnetic gels as well of liquid crystalline elastomers and gels it emerges that piezorheometry is an ideally suited tool to probe the dynamic mechanical properties of both types of systems.

Another important issue, which has not yet been addressed for magnetic gels, but has turned out to be very important for LCEs is the question to what extent the preferred direction (the director in LCEs and the direction of the frozen-in magnetization in anisotropic magnetic gels) can act as an independent macroscopic variable.

In LCEs this topic is closely related to the importance of relative rotations between the director associated with nematic order and the rotations of the polymer network [66, 69]. In nematic LCEs the consequences of relative rotations for the onset of instabilities as well as for the reorientation behavior under an external force such as shear has been studied in quite some detail - compare, for example, Refs. [2, 57, 81, 82]

For anisotropic magnetic gels the study of the question whether the direction of the frozen-in magnetization is a macroscopic variable is a challenge for future experimental investigations. In Sections 18.3 and 18.4 on the macroscopic properties and novel cross-coupling effects we have outlined several possibilities to couple to variations of the preferred direction in magnetic gels. From the experimental investigations carried out so far there appear to be several features, which can possibly influence this question. As discussed in Section II, the experimental results obtained under static external magnetic fields depend sensitively on several factors including the use of iron versus magnetite particles, on the concentration of

magnetic particles, for example $\sim 2\%$ versus $\sim 30\%$, and also on the question whether one uses an aqueous or a polymeric 'solvent'. As a conclusion we stress that the study of the interaction between the magnetic particles and the network clearly needs further investigations statically as well as dynamically.

One of the most remarkable features of nematic side chain LCEs is a plateau-type behavior of the stress-strain curve when a liquid single crystal elastomer (LSCE) is subjected to a mechanical stress perpendicular to the uniform director orientation of the LSCE [83]. Therefore naturally the question arises whether all or any of the anisotropic magnetic gels produced so far also show a plateau-like behavior in the stress-strain curve under analogous conditions as LSCEs.

In this connection it might help to summarize some of the key issues raised and discussed so far concerning the plateau observed for LSCEs. Different models have been put forward for LSCEs by the group around Warner and Terentjev. In their first model nematic LCEs are an anisotropic rubber and the director is not a macroscopic degree of freedom [84]. Here, the plateau in the stress-strain curve is interpreted to be evidence for 'soft elasticity', for which there is no other experimental evidence as yet. The concept of soft elasticity goes back originally to Golubovic and Lubensky [85], who developed it for a novel type of solids (not yet found experimentally). In such a solid one starts from an isotropic phase without an external field [85] and obtains spontaneously a preferred direction. Clearly this concept does not apply to the LSCEs studied experimentally by Küpfer and Finkelmann, since in their case the preferred direction is not at all spontaneous, but rather generated by the crosslinking carried out under an external mechanical stress. It has been shown recently shown recently [86], that one can obtain a plateau in the stress-strain curve without invoking the concept of soft elasticity. Thus one arrives at the conclusion that there is no experimental evidence for "soft elasticity" in the LSCEs as they exist today.

Later on Terentjev and Warner acknowledged that due to the non-spontaneous preferred direction a modification of the concept of "soft elasticity" was necessary; they called it "semi-soft elasticity", since it exhibits the vanishing of the relevant effective elastic coefficient exactly at the beginning and end of the plateau. Such a soft mode behavior (resembling that at a second order phase transition) is in marked contrast to the original "soft elasticity" picture featuring a Nambu-Goldstone scenario, where the relevant linear elastic coefficient is identically zero by symmetry. Nevertheless, soft mode behavior is not a signal of "semi-soft elasticity", but can also be obtained by conventional nonlinear elasticity in combination with nonlinear relative relations [87]. Finally, we point out that the experimental situation regarding the soft mode behavior is still controversial and not yet settled.

ACKNOWLEDGEMENTS

Helmut R. Brand acknowledges the Deutsche Forschungsgemeinschaft for partial support of his work through the Forschergruppe FOR 608 "Nichtlineare Dynamik komplexer Kontinua". Philippe Martinoty thanks the Federation de Recherche CNRS 2863 J. Villermaux for partial support. Helmut R. Brand and Philippe Martinoty acknowledge partial support of their work by PROCOPE 312/pro-ms through the Deutscher Akademischer Austauschdienst and by PAI 02951XJ through the Ministère des Affaires Etrangères.

REFERENCES

[1] Finkelmann, H., Kock, H.J., Rehage, H., Investigations of liquid crystalline polysiloxanes: 3. Liquid crystalline elastomers - a new type of liquid crystalline material, *Makromol. Chem. Rapid Commun.*, 2, 317, 1981.

[2] Brand, H.R., Pleiner, H., Martinoty, P., Selected macroscopic properties of liquid crystalline elastomers, *Soft Matter*, 2, 182, 2006.

[3] Zrinyi, M., Barsi, L., Büki, A., Deformation of ferrogels induced by nonuniform magnetic fields, *J. Chem. Phys.*, 104, 8750, 1996.

[4] Barsi, L., Büki, A., Szabo, D., Zrinyi, M., Gels with magnetic properties, *Progr. Colloid Polym. Sci.*, 102, 57, 1996.

[5] Zrinyi, M., Magnetic field sensitive polymer gels, *Trends in Polymer Science*, 5, 280, 1997.

[6] Zrinyi, M., Barsi, L., Büki, Ferrogel: a new magneto-controlled elastic medium *Polymer Gels and Networks*, 5, 415, 1997.

[7] Zrinyi, M., Barsi, L., Szabo, D. Kilian, H.-G., Direct observation of abrupt shape transition in ferrogels induced by nonuniform magnetic field *J. Chem. Phys.*, 106, 5685, 1997.

[8] Szabo, D., Szeghy, G., Zrinyi, M., Shape transition of magnetic field sensitive polymer gels, *Macromolecules*, 31, 6541, 1998.

[9] Zrinyi, M., Szabo, D., Kilian, H.-G., Kinetics of the shape change of magnetic field sensitive polymer gels, *Polymer Gels and Networks*, 6, 441, 1998.

[10] Mitsumata, T., Ikeda, K., Gong, J.P., Osada, Y., Szabo, D., Zrinyi, M., Magnetism and compressive modulus of magnetic fluid containing gels, *J. Appl. Phys.*, 85, 8451, 1999.

[11] Li, S., John, V.T., Irvin, G.C., Rachakonda, S.H., McPherson, G.L., O'Connor, C.J., Synthesis and magnetic properties of a novel ferrite organogel, *J. Appl. Phys.*, 85, 5965, 1999.

[12] Lebedev, V.T., Torok, G., Cser, L., Buyanov, A.L., Revelskaya, L.G., Orlova, D.N., Sibilev, A.I., Magnetic phase ordering in ferrogels under applied field, *J. Magn. Magn. Mat.*, 201, 136, 1999.

[13] Zrinyi, M., Intelligent polymer gels controlled by magnetic fields, *Colloid Polym. Sci.,*, 278, 98, 2000.

[14] Xulu, P.M., Filipcsei, G., Zrinyi, M., Preparation and responsive properties of magnetically soft poly (N-isopropylacrylamide) gels, *Macromolecules*, 33, 1716, 2000.

[15] Babincova, M., Jeszcynska, D., Sourivong, P., Cicmanec, P., Babinec, P., Superparamagnetic gel as a novel material for electromagnetically induced hyperthermia, *J. Magn. Magn. Mat.*, 225, 109, 2001.

[16] Török, G., Lebedev, V.T., Cser, L., Kali, G., Zrinyi, M., Dynamics of PVA-gel with magnetic macrojunctions, *Physica B*, 297, 40, 2001.

[17] Raikher, Y.L., Rusakov, V.V., Linear orientational magnetodynamics of a ferrogel, *Colloid J.*, 63, 607, 2001.

[18] Jarkova, E., Pleiner, H., Müller, H.-W., Brand, H.R., Hydrodynamics of isotropic ferrogels, *Phys. Rev. E*, 68, 041706, 2003.

[19] Kato, N., Sakai, Y., Kagaya, D., Sekiya, S., Magnetically isotropic - anisotropic change of thermally responsive polymer gels, *Jap. J. Appl. Phys.*, 42, 102-103, 2003.

[20] Hernandez, R., Sarafian, A., Lopez, D., Mijangos, C., Viscoelastic properties of poly(vinyl alcohol) hydrogels and ferrogels obtained through freezing - thawing cycles, *Polymer*, 46, 5543, 2004.

[21] Narita, T., Knaebel, A., Munch, J.-P., Zrinyi, M., Candau, S.J., Microrheology of chemically crosslinked polymer gels by using diffusing-wave spectroscopy, *Macromol. Symp.*, 207, 17, 2004.

[22] Teixeira, A.V., Licinio, P., Local deformations of ferrogels induced by uniform magnetic fields, *J. Magn. Magn. Mat.*, 289, 126, 2005.

[23] Wang, G., Tian, W.J., Huang, J.P., Response of ferrogels to an AC magnetic field, *J. Phys. Chem. B*, 110, 10738, 2006.

[24] Filipcsei, G., Szilagyi, A., Csetneki, I., Zrinyi, M., Comparative study on the collapse transition of poly (N-Isopropylacrylamide) gels and magnetic nanoparticles loaded poly (N-isopropylacrylamide) gels, *Macromol. Symp.*, 239, 130, 2006.

[25] Liu, T.-Y., Hu, S.-H., Liu, T.-Y., Liu, D.-M., Chen, S.-y., Magnetic-sensitive behavior of intelligent ferrogels for controlled release of drug, *Langmuir*, 22, 5974, 2006.

[26] Bentivegna, F., Ferré, J., Nyvlt, M., Jamet, J.P., Imhoff, D., Canva, M., Brun, A., Veillet, P., Visnovsky, S., Chaput, F., Boilot, J.P., Magnetically textured $\gamma-Fe_2O_3$ nanoparticles in a silica gel matrix: structural and magnetic properties, *J. Appl. Phys.*, 83, 7776, 1998.

[27] Bentivegna, F., Nyvlt, M., F., Ferré, J., Jamet, J.P., Brun, A., Visnovsky, S., Urban, R., Magnetically textured $\gamma-Fe_2O_3$ nanoparticles in a silica gel matrix: optical and magneto-optical properties, *J. Appl. Phys.*, 85, 2270, 1999.

[28] Uritani, M., Hamada, A., A simple and inexpensive dot-blotter for immunoblotting, *Biochem. Education*, 27, 169, 1999.

[29] Mitsumata, T., Furukawa, K., Juliac, E., Iwakura, K., Koyama, K., Compressive modulus of ferrite containing polymer gels, *Int. J. Mod. Phys. B*, 16, 2419, 2002.

[30] Mitsumata, T., Juliac, E., Furukawa, K., Iwakura, K., Taniguchi, T., Koyoma, K., Anisotropy in longitudinal modulus of polymer gels containing ferrites, *Macromol. Rapid Commun.*, 23, 175, 2002.

[31] Wilson, M.J., Fuchs, A., Gordaninejad, F., Development and characterization of magnetorheological polymer gels, *J. Appl. Polym. Sci.*, 84, 2733, 2002.

[32] Horvath, A.T., Klingenberg, D.J., Shkel, Y.M., Determination of rheological and magnetic properties for magnetorheological composites via shear magnetization measurements, *Int. J. Mod. Phys. B*, 16, 2690, 2002.

[33] Ginder, J.M., Clark, S.M., Schlotter, W.F., Nichols, M.E., Magnetostrictive phenomena in magnetorheological elastomers, *Int. J. Mod. Phys. B*, 16, 2412, 2002.

[34] Schlotter, W.F., Cionca, C., Paruchuri, S.S., Cunningham, J.B., Dufresne, E., Dierker, S.B., Arms, D., Clarke, R., Ginder, Nichols, M.E., The dynamics of magnetorheological elastomers studied by synchrotron radiation speckle analysis, *Int. J. Mod. Phys. B*, 16, 2426, 2002.

[35] Bellan, C., Bossis, G., Field dependence of viscoelastic properties of MR elastomers, *Int. J. Mod. Phys. B*, 16, 2447, 2002.

[36] Szabo, D., Zrinyi, M., Nonhomogeneous, non-linear deformation of polymer gels swollen with magneto-rheological suspensions, *Int. J. Mod. Phys. B*, 16, 2616, 2002.

[37] Davis, L.C., Model of magnetorheological elastomers, *J. Appl. Phys.*, 85, 3348, 1999.

[38] Collin, D., Auernhammer, G.K., Gavat, O., Martinoty, P., Brand, H.R., Frozen-in magnetic order in uniaxial magnetic gels: Preparation and physical properties, *Macromol. Rapid Commun.*, 24, 737, 2003.

[39] Varga, Z., Feher, J., Filipcsei, G., Zrinyi, M., Smart nanocomposite polymer gels, *Macromol. Symp.*, 200, 93, 2003.

[40] Varga, Z., Filipcsei, G., Szilagyi, A., Zrinyi, M., Electric and magnetic field-structured smart composites, *Macromol. Symp.*, 227, 123, 2005.

[41] Varga, Z., Filipcsei, G., Zrinyi, M., Smart composites with controlled anisotropy, *Polymer*, 46, 7779, 2005.

[42] Varga, Z., Filipcsei, G., Zrinyi, M., Magnetic field sensitive functional elastomers with tunable elastic modulus, *Polymer*, 47, 227, 2006.

[43] Csetneki, I., Filipcsei, G., Zrinyi, M., Smart nanocomposite polymer membranes with on/off switching control, *Macromolecules*, 39, 1939, 2006.

[44] Hajsz, T., Csetneki, I., Filipcsei, G., Zrinyi, M., Swelling kinetics of anisotropic filler loaded PDMS networks, *Phys. Chem. Chem. Phys.*, 8, 977, 2006.

[45] Auernhammer, G.K., Collin, D., Martinoty, P., Viscoelasticity of suspensions of magnetic particles in a polymer: Effect of confinement and external field, *J. Chem. Phys.*, 124, 204907, 2006.

[46] Lattermann, G., Krekhova, M., Thermoreversible ferrogels, *Macromol. Rapid Commun.*, 27, 1373, 2006; 1968, 2006.

[47] Bohlius, S., Brand, H.R., Pleiner, H., Macroscopic dynamics of uniaxial magnetic gels, *Phys. Rev. E*, 70, 061411, 2004.

[48] Bohlius, S., Brand, H.R., Pleiner H., Surface waves and Rosensweig instability in isotropic ferrogels, *Z. Physik. Chemie*, 220, 97, 2006.

[49] Bohlius, S., Pleiner, H., Brand, H.R., Pattern formation in ferrogels: analysis of the Rosensweig instability using the energy method, *J. Phys. Cond. Matter*, 18, S2671, 2006.

[50] Pleiner, H., Brand, H.R., Hydrodynamics and Electrohydrodynamics of Nematic Liquid Crystals, in *Pattern Formation in Liquid Crystals*, A. Buka and L. Kramer, Eds., Springer, New York, p.15 ff (1996).

[51] See for example: Treloar, L.R.G., *The Physics of Rubber Elasticity*, Oxford, Clarendon Press, 1949.

[52] Gallani, J.-L., Hilliou, L., Martinoty, P., Doublet, F., Mauzac, M., Mechanical behavior of side-chain liquid crystalline networks, *J. Phys. II (France)*, 6, 443, 1996.

[53] Weilepp, J., Stein, P., Aßfalg, N., Finkelmann, H., Martinoty, P., Brand, H.R., Rheological properties of mono-and polydomain liquid crystalline elastomers exhibiting a broad smectic-A phase, *Europhys. Lett.*, 47, 508, 1999.

[54] Weilepp, J., Zanna, J.J., Aßfalg, N., Stein, P., Hilliou, L., Mauzac, M., Finkelmann, H., Brand, H.R., Martinoty, P., Rheology of liquid crystalline elastomers in their isotropic and smectic-A state, *Macromolecules*, 32, 4566, 1999.

[55] Stein, P., Aßfalg, N., Finkelmann, H., Martinoty, P., Shear modulus of polydomain, mono-domain and non-mesomorphic side-chain elastomers: influence of the nematic order, *Eur. Phys. J. E*, 4, 255, 2001.

[56] Zanna, J.J., Stein, P., Marty, J.D., Mauzac, M., Martinoty, P., Influence of molecular parameters on the elastic and viscoelastic properties of side-chain liquid crystalline elastomers, *Macromolecules*, 35, 5459, 2003.

[57] Martinoty, P., Stein, P., Finkelmann, H., Pleiner, H., Brand, H.R., Mechanical properties of monodomain side-chain nematic elastomers, *Eur. Phys. J. E*, 14, 311, 329, 339, 2004.

[58] Rogez, D., Francius, F., Finkelmann, H., Martinoty, P., Shear mechanical anisotropy of side chain liquid-crystal elastomers: influence of sample preparation, *Eur. Phys. J. E*, 20, 369, 2006.

[59] Rogez, D., Brandt, H., Finkelmann, H., Martinoty, P., Shear mechanical properties of main chain liquid crystalline elastomers, *Macromol. Chem. Phys.*, 207, 735, 2006.

[60] Martinoty, P., Hilliou, L., Mauzac, M., Benguigui, L., Collin, D., Side-chain liquid-crystal polymers: gel-like behavior below their gelation points, *Macromolecules*, 32, 1746, 1999.

[61] Collin, D., Martinoty, P., Dynamic macroscopic heterogeneities in a flexible linear polymer melt, *Physica A*, 320, 235, 2003.

[62] Collin, D., Martinoty, P., Commentary on Solid-like rheological response of non-entangled polymers in the molten state by H. Mendil et al, *Eur. Phys. J. E*, 19, 87-98, 2006.

[63] Collin, D., Lavalle, P., Garza, J.M., Voegel, J.C., Schaaf, P., Martinoty, P., Mechanical properties of cross-linked hyaluronic acid/poly-(L-lysine) multilayer films, *Macromolecules*, 37, 10195, 2004.

[64] Temmen, H., Pleiner, H., Liu, M., and Brand, H.R., Convective nonlinearity in non-Newtonian fluids, *Phys. Rev. Lett.* 84, 3228, 2000.

[65] Landau, L.D. and Lifshitz, I. M., *Electrodynamics of Continuous Media* (Addison-Wesley, Reading, MA, 1960).

[66] De Gennes, P.G., *Weak nematic gels*, p.231 ff in *Liquid Crystals of One- and Two-Dimensional Order*, Helfrich, W., Heppke, G., Eds., Springer, New York, 1980.

[67] Menzel, A.M., Pleiner, H., and Brand, H.R., Nonlinear relative rotations in liquid crystalline elastomers, *J. Chem. Phys.*, 126, 234901, 2007.

[68] Graham, R., Hydrodynamics of He-3 in anisotropic A phase, *Phys. Rev. Lett.* 33, 1431, 1974.

[69] Brand, H.R., Pleiner, H., Electrohydrodynamics of nematic liquid crystalline elastomers, *Physica A*, 208, 359, 1994.

[70] Jarkova, E., Pleiner, H., Müller, H.-W., and Brand, H.R., Macroscopic dynamics of ferronematics, *J. Chem. Phys.* 118, 2422, 2003.

[71] Ryskin, A., Müller, H.-W., and Pleiner, H., Hydrodynamic instabilities in ferronematics, *Eur. Phys. J. E* 11, 389, 2003.

[72] du Trémolet de Lacheisserie, E., *Magnetostriction – Theory and Applications of Magnetoelasticity*, (CRC Press, Boca Raton, 1993).

[73] Nikitin, L.V. , Mironova, L.S., Stepanov, G.V., and Samus, A.N., The influence of a magnetic field on the elastic and viscous properties of magnetoelastics, *Polym. Sci., Ser. A Ser. B* 43, 443, 2001.

[74] Harden, J.L., Pleiner, H., and Pincus, P.A., Hydrodynamic surface modes on concentrated polymer solutions and gels, *J. Chem. Phys.* 94, 5208, 1991.

[75] Rosensweig, R.E., *Ferrohydrodynamics*, Cambridge University Press, Cambridge, (1985).

[76] Jackson, J.D., *Classical Electrodynamics*, 2nd edn., John Wiley & Sons, Inc., (1999).

[77] Gailitis, A., Formation of hexagonal pattern on surface of a ferromagnetic fluid in an applied magnetic field, *J. Fluid Mech.* 82, 401, 1977.

[78] Friedrichs, R. and Engel, A., Pattern and wavenumber selection in magnetic fluids, *Phys. Rev. E*, 64, 021406, 2001.

[79] Bohlius, S., Brand, H.R., and Pleiner, H., Amplitude equation for the Rosensweig instability, *Prog. Theor. Phys. Suppl.*, 175, 27, 2008; The amplitude equation for the Rosensweig instability in magnetic fluids and gels, submitted for publication, 2008.

[80] Brand, H.R., Finkelmann, H., Physical Properties of Liquid Crystalline Elastomers, in *Handbook of Liquid Crystals*, J.W. Goodby et al., Eds., Wiley, New York, Vol.3, p.277 ff (1998).

[81] Mueller, O., Brand, H.R., Undulation versus Frederiks instability in nematic elastomers in an external electric field, *Eur. Phys. J. E*, 17, 53, 2005.

[82] Weilepp, J., Brand, H.R., Director reorientation in nematic liquid single crystal elastomers, *Europhys. Lett*, 34, 495, 1996; *Europhys. Lett*, 37, 499, 1997.

[83] Küpfer, J., Finkelmann, H., Liquid crystal elastomers - influence of the orientational distribution of the cross-links on the phase behavior and reorientation processes, *Macromol. Chem. Phys.*, 195, 1353, 1994.

[84] Warner, M., Terentjev, E.M., *Liquid Crystal Elastomers*, Oxford University Press, Oxford, 2003; Warner, M., New elastic behavior arising from the unusual constitutive relation of nematic solids, J. Mech. Phys. Sol., 47, 1355, 1999.

[85] Golubovic, L., Lubensky, T.C., Nonlinear elasticity of amorphous solids, *Phys. Rev. Lett.*, 63, 1082, 1989.

[86] A.M. Menzel, H. Pleiner, and H.R. Brand, Response of prestretched nematic elastomers to external fields, *Eur. Phys. J. E* 30, 371, 2009.

[87] Kundler, I., Finkelmann, H., Strain-induced director reorientation in nematic liquid single crystal elastomers, *Macromol. Rapid Commun.*, 16, 679, 1995.